POLITECNICO DI TORINO

Master's Degree in **BUILDING ENGINEERING**

3D Rockfall Analysis

The case study of Varallo (VC,Italy)

Candidate: Daniyal Farzaneh

Supervisors: Proff. Monica Barbero
Dr. Maria Lia Napoli

A.Y. 2024-2025

Abstract

This Thesis addresses the issue of rockfall instability and its mitigation, focusing specifically on the case study of a slope in **Varallo (VC, North-West Italy)**. This region has been prone to rockfall phenomena over the years, with significant consequences for the road situated at its base. Through the application of **Rocfall 3D** using the **Rock Science Simulation Tool**, the study evaluates the rockfall risk and proposes strategies to enhance the safety of the infrastructure.

The analysis begins by estimating the rock block volume for the simulations, referred to as the **design block**, using various methodologies available in the literature. These include simpler methods based on blocks already fallen at the slope's base, as well as more complex statistical analysis. Subsequently, the parameters involved in the trajectory simulations are defined through a **back analysis** of a rockfall event that occurred in **November 2023**.

Further simulations are carried out considering multiple scenarios, such as varying block volumes. The study concludes with the proposal of **different mitigation interventions** for the rockfall hazard based on the outcomes of the trajectory analyses, providing recommendations for improving the safety of the road and surrounding areas.

Table of Contents

1) Introduction

Rockfalls are a common hazard in mountainous and hilly terrains, typically resulting from a variety of natural processes such as erosion, weathering, seismic activity, and rainfall. These events, where rock masses break away from slopes and descend rapidly, pose significant risks to both infrastructure and human life.[4]
The unpredictability of rockfall events, combined with the challenging and often steep topography of mountainous regions, makes them a complex phenomenon to study and mitigate.[2][4]

Figure 1. *Rock fall occurred near Valtopina, Umbria*

1. 2) Rockfall Triggering Factors

Rockfalls are primarily triggered by a combination of structural and environmental factors. Structurally, rockfalls occur when a loose mass of rock on a slope becomes unstable due to a variety of mechanisms, such as jointing or the presence of pre-existing fractures in the rock mass. The physical and chemical weathering of rocks, along with the freeze–thaw cycles, can weaken the cohesion of these rock masses, making them more susceptible to failure.[2][3]

Environmental factors like heavy rainfall, rapid temperature fluctuations, and seismic shaking are also significant triggers. These events can increase pore water pressure, causing further weakening of the rock structure. Additionally, human activity such as excavation, construction, and the use of heavy machinery can contribute to destabilizing slopes. Furthermore, any vibration, whether caused by seismic activity or human-made sources, can initiate a rockfall, often with significant consequences.[4]

Figure 2*. Rockfall in South Tyrol, Italy 21 may 2023*

1. 3) Factors Affecting Rockfall Behavior

Once a rockfall has been initiated, the subsequent motion of the rock is influenced by various factors including slope geometry, material properties, and surface conditions.
The **slope geometry**, including factors such as angle, length, and surface roughness, plays a crucial role in the velocity and direction of the falling rock. For example, steep slopes typically accelerate rocks more quickly, while surface irregularities can change the path of the rock, causing it to bounce or roll.[4]

The **material properties** of the rock and the surface it interacts with further affect the behavior of the rock during its descent. Harder rocks, for example, tend to travel further than softer rocks, and their shape and size contribute to how much kinetic energy they carry. Larger rocks generally possess more energy and travel further before coming to a stop.[2][4]

Human interventions, such as the construction of retaining walls or roads, can also impact rockfall behavior by creating artificial pathways that alter the natural motion of falling rocks.[8] Similarly, the presence of vegetation may slow down the movement of smaller blocks but may not prevent larger rocks from continuing their path down the slope.[3]
The conceptual model illustrated in [**Figure 3]** summarizes the typical kinematic domains of a rockfall event, describing the transition from the release area to the final deposition zone. It highlights the key geometrical parameters—such as the reach angle (α) and shadow angle (β)—that control the maximum runout distance of falling blocks.

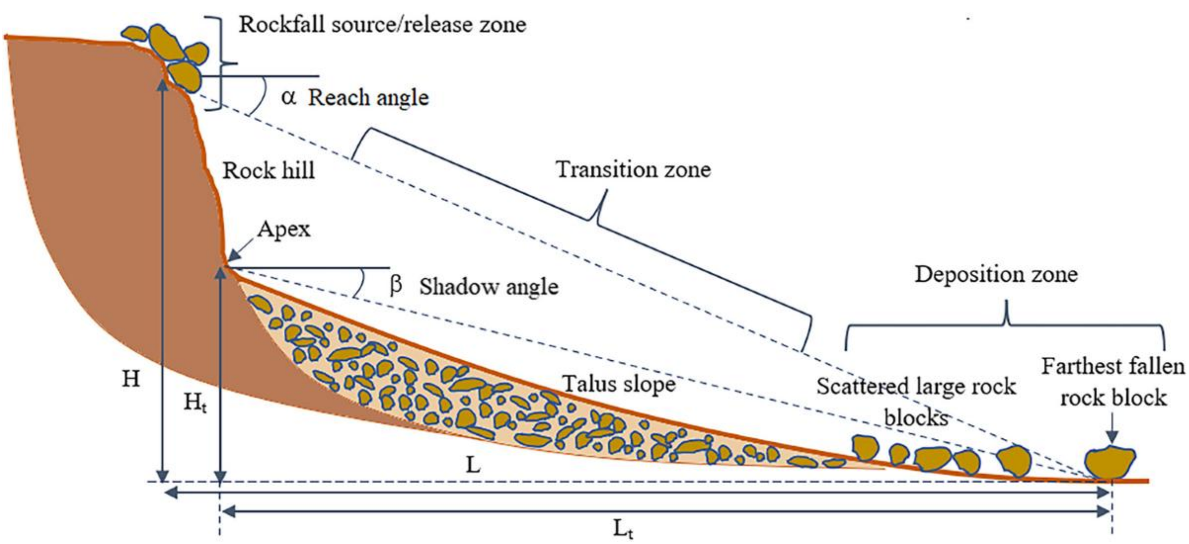

Figure 3. *Mechanics and modelling approaches of rockfall [9]*
*source: **Arabian Journal of Geosciences***

1. 4) Rockfall Failure Mechanism

The mechanism by which a rock mass fails and triggers a rockfall is determined by its structural properties. Rock masses are typically fractured into discrete blocks by discontinuities, such as joints or faults. The orientation of these discontinuities with respect to the slope is critical in determining whether a rock mass will fail by sliding, toppling, or other failure modes. [3]

1. **Planar failure** occurs when a block of rock slides along a plane of weakness that is aligned with the slope, while **wedge failure** happens when two intersecting joint sets form a wedge that can detach and slide down the slope.
2. **Toppling failure** is associated with the rotation of blocks that are constrained at the bottom but loose at the top, often occurring on steep slopes with joints or fractures dipping away from the slope face.

The different mechanisms through which a rock slope may fail are illustrated in [**Figure 4]** showing the most common failure modes—including planar, wedge, toppling and circular failures—each governed by the orientation and interaction of structural discontinuities.

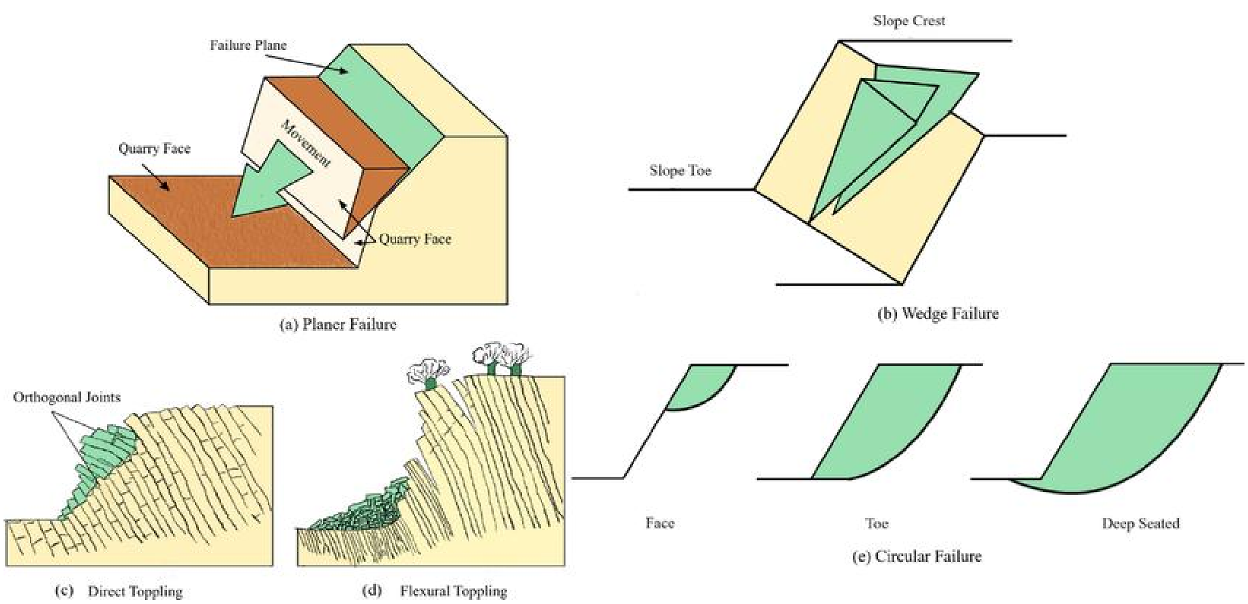

Figure 4. *Types of slope failure; a planar, b wedge, c & d toppling, e circular[4]*

.

1. 5) Rockfall Hazard Assessment

Rockfall hazard assessment is a critical aspect of evaluating the risk posed by rockfalls to infrastructure and human life. It involves analyzing three key components: **susceptibility**, **frequency**, and **propagation**.[1][5]

- **Susceptibility** refers to the likelihood that a rockfall will occur in a specific area based on local terrain conditions, including the slope angle, material properties, and existing fractures.[1]
- **Frequency** pertains to the temporal occurrence of rockfalls, often determined through statistical analysis of past events and their recurrence intervals.[5]
- **Propagation** describes the trajectory and runout distance of falling rocks, which is influenced by the slope's geometry and surface characteristics.[5]

The conceptual scheme shown in [**Figure 5]** illustrates the typical spatial subdivision of a rockfall path, including the release zone, the transition zone and the final deposition area. This representation highlights how block motion evolves downslope and how the shadow angle governs the maximum runout distance.

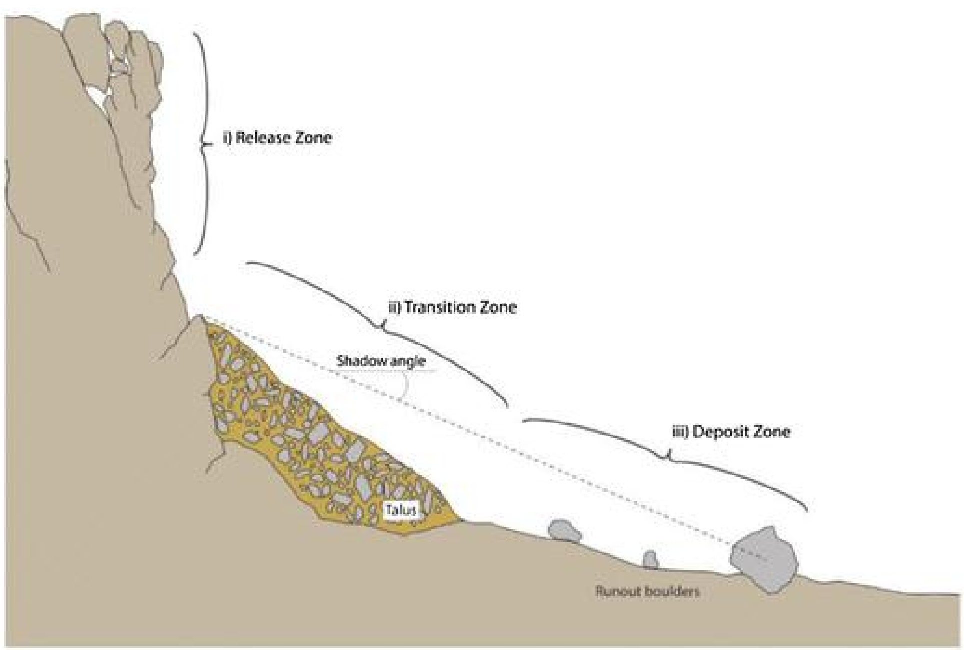

Figure 5. *Laser Scanning Systems and Techniques in Rockfall[4]*

2) The Rockfall Susceptibility Index to Failure (SIF)

To estimate how likely a rock block is to become unstable and detach from a slope, the Rockfall Susceptibility Index to Failure (SIF) was introduced as a semi-quantitative method based on a combination of geological and environmental factors. These factors describe the main causes that make a slope prone to failure and were selected through an extensive review of the scientific literature.[1][2]

For practical use, the factors were grouped into three main categories:

- The first group (Table A) includes **general predisposing and triggering factors**, which can be found in any type of terrain, regardless of the local environment.
- The other two groups (Tables B1 and B2) describe conditions that are specific either to **mountainous areas (B1)** or to **coastal–marine settings (B2)**.
  Since a site can belong to only one of these two environments, the B1 and B2 tables are considered *mutually exclusive*.

Each factor ***f*** is divided into classes according to its degree of influence on rockfall initiation, and a numerical score ***P*** is assigned. The scores usually range from 0 (very low susceptibility) to 3 (very high susceptibility), representing how strongly each factor contributes to potential instability.

In some special cases—such as when effective stabilization or protection works are present—negative scores (up to −1) can be applied to reduce the overall susceptibility, since these structures lower the probability of detachment.

Once all relevant factors are evaluated, the SIF index is calculated by combining their weighted contributions. The formula slightly differs depending on whether the site is located in a mountain or coastal–marine environment.[1][2]

For **mountain environments**, the SIF is defined as:

$$SIF = \frac{\sum(P_{f,A} + P_{f,B1}) - \sum\min\,(P_{f,A} + P_{f,B1})}{\sum\max\,(P_{f,A} + P_{f,B1}) - \sum\min\,(P_{f,A} + P_{f,B1})}$$

For **coastal–marine environments**, it is expressed as:

$$SIF = \frac{\sum(P_{f,A} + P_{f,B2}) - \sum\min\,(P_{f,A} + P_{f,B2})}{\sum\max\,(P_{f,A} + P_{f,B2}) - \sum\min\,(P_{f,A} + P_{f,B2})}$$

where:

- $P_{f,A}$ is the weight assigned to each factor in **Table A[Figure 7]**
- $P_{f,Bi}$ (where *i* = 1 or 2) is the weight assigned to the factors in **Table B1** or **Table B2** [**Figure 7**]
- $\sum\min\,(P_{f,A} + P_{f,Bi})$ represents the sum of the **minimum possible weights** for all factors;
- $\sum\max\,(P_{f,A} + P_{f,Bi})$ represents the sum of the **maximum possible weights**.

If one or more parameters cannot be properly assessed—such as when visibility of the slope is limited—the corresponding minimum and maximum values are excluded from the computation so that they do not distort the final index.

In essence, the SIF equation normalizes the total influence of all instability factors, transforming it into a dimensionless number between **0 and 1**. Values close to 1 indicate a high probability of rock detachment, while values near 0 correspond to stable conditions.

This formulation allows for a consistent comparison between different areas of a slope and provides a solid quantitative basis for identifying the most hazardous zones.

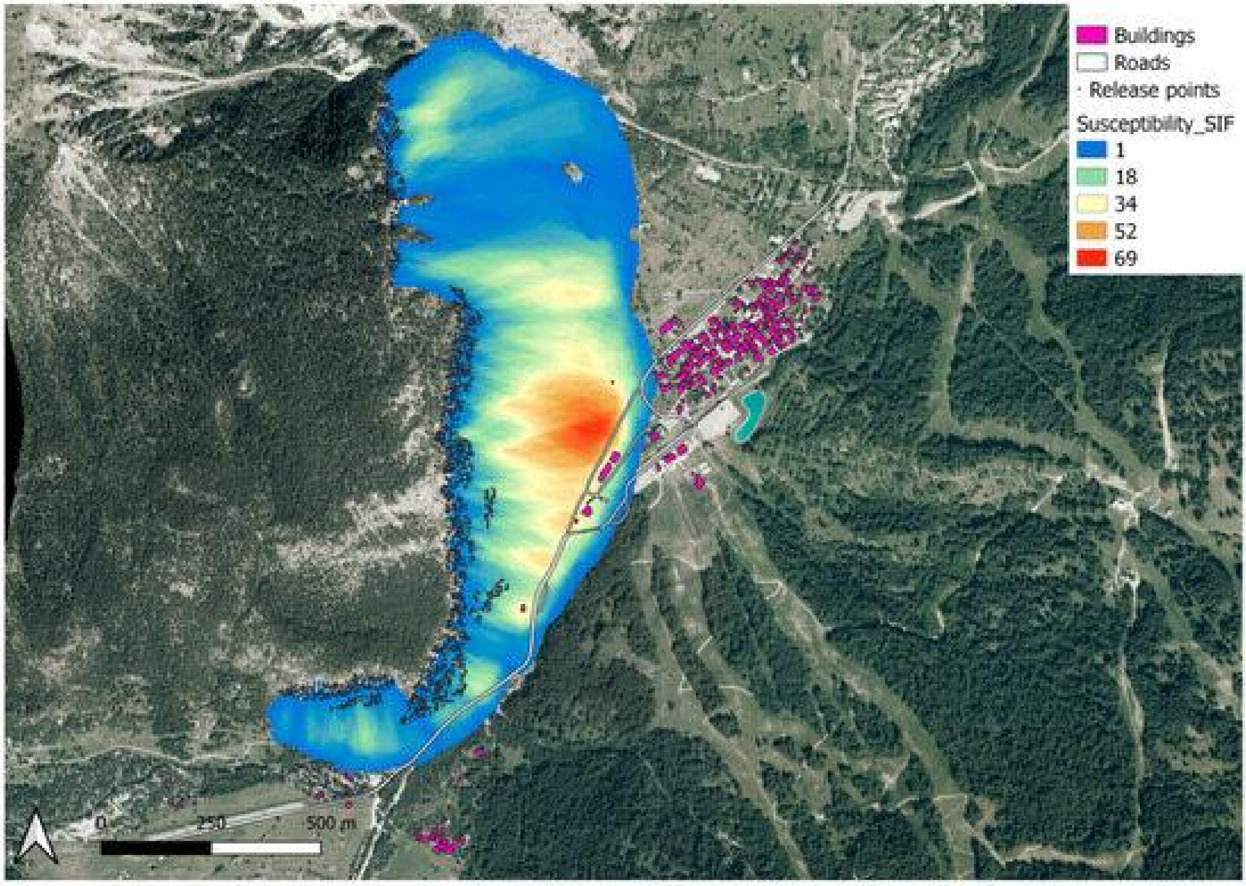

Figure 6. *A Novel Approach to Assess the Influence of Rockfall Source Areas:*

The Case Study of Bardonecchia (Italy)

TABLE A - General							
WEIGHT, P **PARAMETER**	**-1**	**-0.5**	**0**	**0.5**	**1**	**2**	**3**
Slope angle			<15°	15°-30°	30°-45°	45°-70°	>70°
Rock mass structural conditions*			Massive rock with no or a few discontinuities (Jn=0.5÷1)	One set of discontinuities (Jn =2÷3)	Two sets of discontinuities (Jn =4÷6)	Three sets of discontinuities, rock mass subdivided into small cubes (Jn =9÷12)	More than three sets of discontinuities, highly fractured rock mass (Jn =15÷20)
Discontinuity aperture *			Closed or slightly opened		1 mm - 1 cm	1 cm - 10 cm	>10 cm
Stability conditions *			Stable		Partially stable	Unstable	
Fracturing degree of the rock mass **			Low		Medium	High	Very high
Expected rockfall events			Few events (1/10 years) - no rockfall scars		Occasional events (3/year)	Many events-visible rockfall scars (6/year)	Numerous and frequent events (9/year)
Precipitation			Low		Moderate	Intense	
Aggravating conditions							
Unstable blocks and/or overhanging sectors			None			Present	
Geological singularities (presence of faults, low resistance interlayers, heterogeneity, etc.)			None		Present		
Seepage/water			No/a few water seeps on slope		Numerous water seeps on slope		
Lateral or foot torrential erosion			None		Present		
Seismicity			Low		Moderate	High	
Stabilization works	Fully efficient/ effective	Partially efficient/ effective	None				
TABLE B1 - Mountain environment							
Lithology			Good quality rock			Soft rock	
Freeze–thaw cycles			None		Present		
TABLE B2 - Marine environment							
Slope orientation			Favorable (roughly shore-normal storm wave fronts)		Adverse (shoreline subparallel to main storm wave fronts)		
Elevation of the source area a.s.l.			High enough not to be affected by the erosive/unstable effects caused by waves, sea spray and tides		Not high enough to exclude erosive/unstable effects caused, even indirectly, by waves, sea spray and tides	Low enough to be affected by the erosive/unstable effects caused by waves, sea spray and tides	
Lithology and sensitivity to the erosive action of the sea			Good quality rocks (metamorphic, volcanic, etc.)		Medium quality rocks (limestones,sandstones conglomerates, etc.)	Rocks of low quality or sensitive to the marine environment	
Tidal effect			Not applicable, altitude of the source area sufficiently high	Low oscillations	Significant oscillations		
Wave energy			Not applicable, altitude of the source area sufficiently high	Moderate	High	Very high	
Cliff foot directly exposed to waves/tides			Not applicable - Protective beaches or engineering structures		No protective beaches or engineering structures		
Coastal retreat rate *			Very limited/limited		Significant		
Karst features			None		Limited	Significant	

Figure 7*. Parameters controlling rock blocks failure probability: classification and relative scores.*
The SIF index can be obtained by combining the weights assigned to the parameters of Tables A+B1 in the case of mountain environment, or A+B2 in the case of coastal-marine environment.

3) Site Characterization

3.1) Geographical and Geological Setting

The study area is located in the municipality of Varallo, within the Valsesia Valley (Vercelli province, Piedmont Region, Northern Italy). This sector of the Sesia Valley is characterized by steep rocky slopes that frequently experience rockfall events, mainly affecting the provincial road that runs along the valley floor and several nearby infrastructures.[1]

Coordinates (WGS-84):
Latitude = 45° 48' 50" N (≈ 45.8139°)
Longitude = 8° 15' 30" E (≈ 8.2583°)

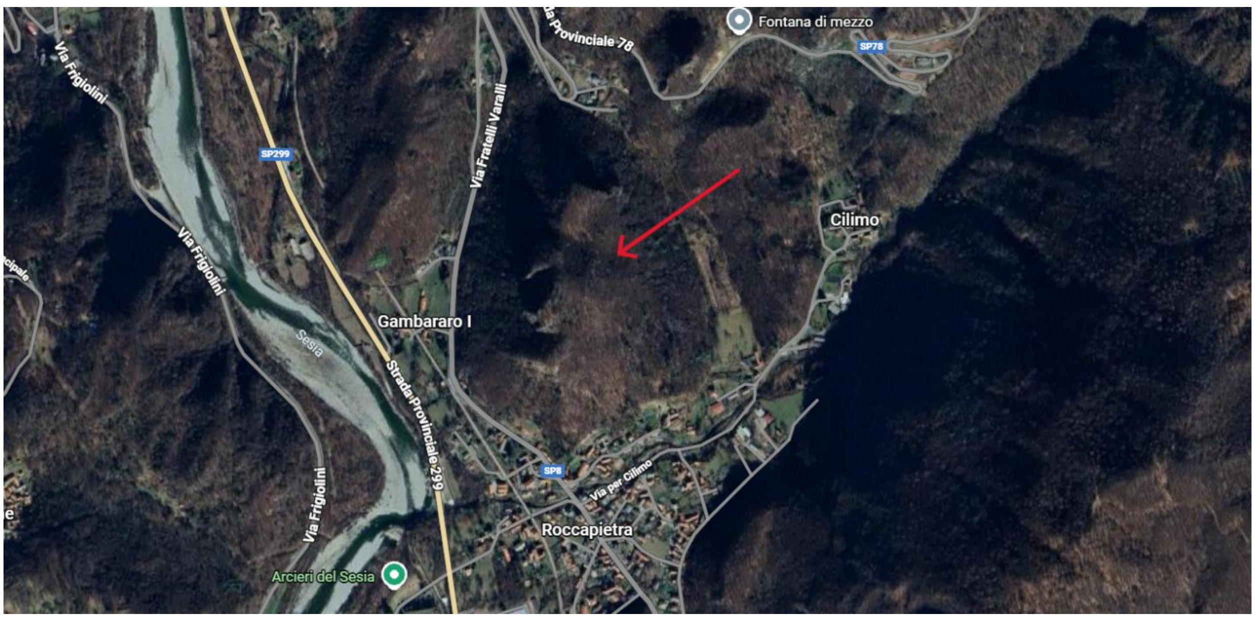

Figure 8. *Exact location of Roccapietra Varalo, Vercelli*

Varallo lies within the central segment of the Ivrea–Verbano Zone, a geological unit belonging to the Southern Alps. The rock slope investigated in this study mainly consists of kinzigites, which are coarse-grained paragneisses of pre-Ordovician age. These rocks have undergone high-grade Variscan metamorphism, leading to the formation of minerals such as biotite, sillimanite, cordierite, garnet, quartz, muscovite, plagioclase, and K-feldspar.[1]

Figure 9. *Samples of kinzigites*

Partial melting (anatexis) processes generated pockets and veins of granitic composition, giving the rock a migmatitic texture. Locally, the secondary lithology includes the Roccapietra granite, a biotite–hornblende granodiorite belonging to the local granitic pluton. Dioritic rocks from the Appinitic suite of Lower Permian age are also present in minor amounts.

The structural setting of the slope shows a dense network of joints, foliation planes, and fractures, often favorably oriented with respect to the slope face, thus promoting potential rock detachments. The overall geological and structural conditions make the site highly susceptible to instability phenomena, particularly along the southwestern and central-western sectors of the slope.[1]

3.2) Rockfall History and Previous Events

The Varallo slope has been affected by several rockfall events over the past decades. According to the Regional Landslide Inventory (SIFRAP) of the Piedmont Region, two major events (IDs 2001390 and 20033600) have been recorded in the area.

In November 2023, a significant rockfall event occurred, involving a kinzigite block of approximately 3 m^3, which detached from the upper part of the slope and impacted the road at its base, causing considerable damage.

Following this event, detailed field surveys and photogrammetric inspections were conducted to assess the stability of the remaining rock masses. A large number of unstable blocks were identified, particularly in the southern sector of the slope, where subsequent rock-scaling interventions were carried out by professional climbers to remove potentially unstable fragments.

In addition, two rockfall barriers, installed in the 1990s and later in 2012, were found to have successfully stopped tens of falling blocks, providing valuable data for the estimation of block sizes and trajectories. These historical and observational data were essential for the calibration of both the Rocfall3D simulation and the susceptibility indexes.[1]

***Figure 10**.a) detachment niche located on the Barbavara castle rock slope;*
b) kinzigite rock block of about 3 m3 that detached in
c) road damaged by the rock collapse[1]

3.3) Field Survey and Data Collection

A series of **in-situ surveys** and **geospatial analyses** were carried out to prepare the input data required for the 3D simulation and susceptibility mapping.
The surveys aimed to:

1. Evaluate the **rock mass conditions** and identify major discontinuities.
2. Measure and record the **size, volume, and position** of previously detached rock blocks.
3. Assess the **efficiency and damage state** of the existing mitigation structures.

The **Digital Terrain Model (DTM)** of the area, provided by regional authorities, was processed in **QGIS** to obtain key morphological parameters such as **slope angle, aspect, and curvature**. The DTM resolution was high enough to allow the accurate delineation of the main geomorphological features influencing rockfall behavior.[1]
The Digital Terrain Model used for the geomorphological analysis is shown in [**Figure 11**], highlighting the extent of the study area as imported and visualized within the QGIS environment.

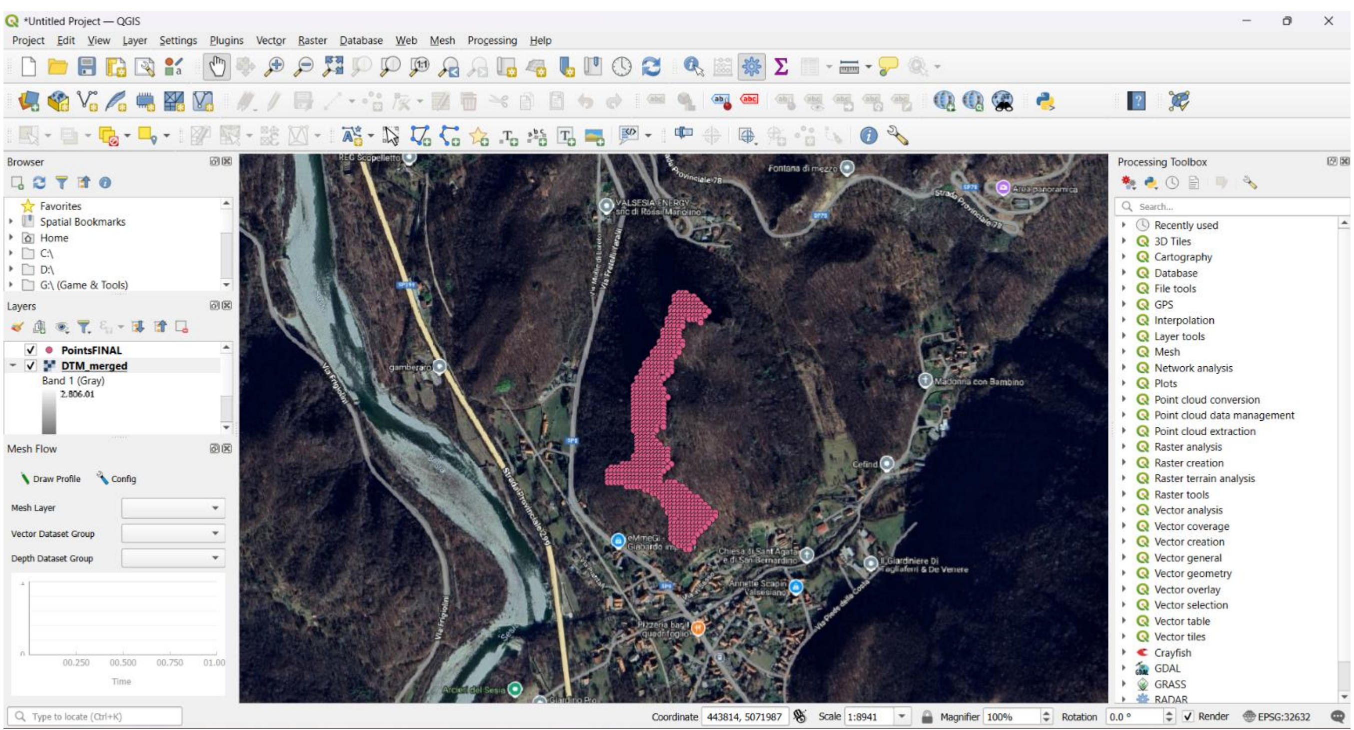

***Figure 11**. DTM view in QGIS*

4. Methodology and Software Tools

4.1 Overview of the Adopted Methodology

The numerical analysis performed in this study combines both **GIS-based modeling** and **3D physical simulation** in order to evaluate the rockfall hazard affecting the Varallo slope.
Two main software environments were used:

- **QGIS**, an open-source Geographic Information System employed for spatial analysis and susceptibility mapping;
- **Rocfall 3D**, a 3D numerical simulator developed by Rocscience, used to reproduce the kinematic behavior of falling rock blocks and to estimate the corresponding impact energies and runout distances.[6]
- **Rockyfor3D**, a physically based rockfall model that includes soil–block interaction, vegetation influence, and probabilistic runout estimation, complementing the purely kinematic simulations of Rocfall 3D [5].

The integration between these two tools allows a multi-scale investigation of the phenomenon: while QGIS provides a territorial-level susceptibility analysis based on topographic and geological parameters, Rocfall 3D allows a detailed understanding of the physical motion and energy distribution of individual blocks.[1][6]

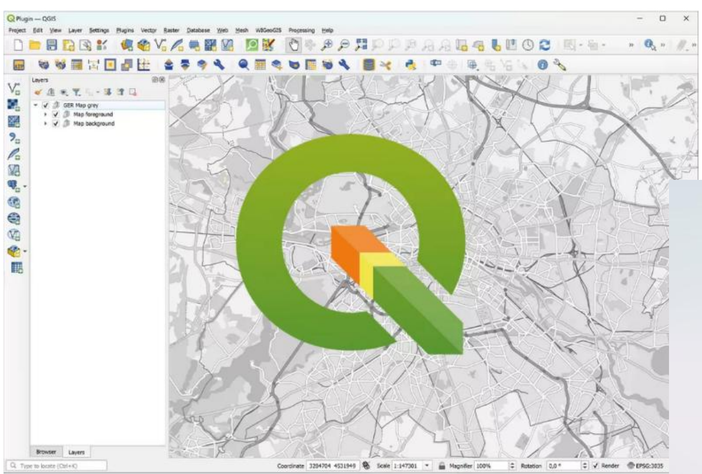

Figure 12. *QGIS Software*

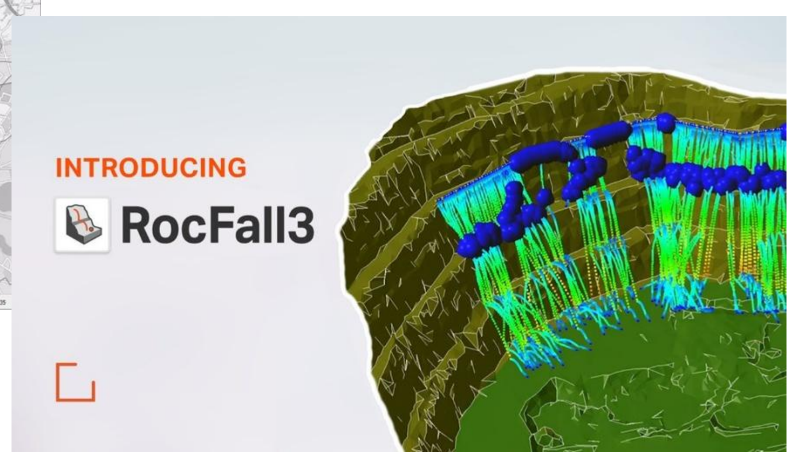

Figure 13. *Rocfall 3D Software*

4. 2) QGIS Workflow and procedure

4.2.1) Workflow Overview

The GIS-based part of this study was carried out in **QGIS**, where the complete workflow included:

1. Preprocessing the **Digital Terrain Model (DTM)** and vector data.
2. Deriving topographic parameters (slope, aspect, curvature).
3. Defining and importing the **source points**.
4. Running the **QPROTO** plugin to simulate potential runout zones using the *Cone Method*.
5. Generating and exporting the final susceptibility and impact maps.

4.2.2) Data Preparation in QGIS

The regional **Digital Terrain Model (DTM)**, provided as DTM_merged.tif, was imported into QGIS using:
Layer → Add Layer → Add Raster Layer which we can see in [**Figure 14**]
All layers were projected into a common coordinate system (**EPSG:4326 – WGS84**) to ensure spatial consistency.

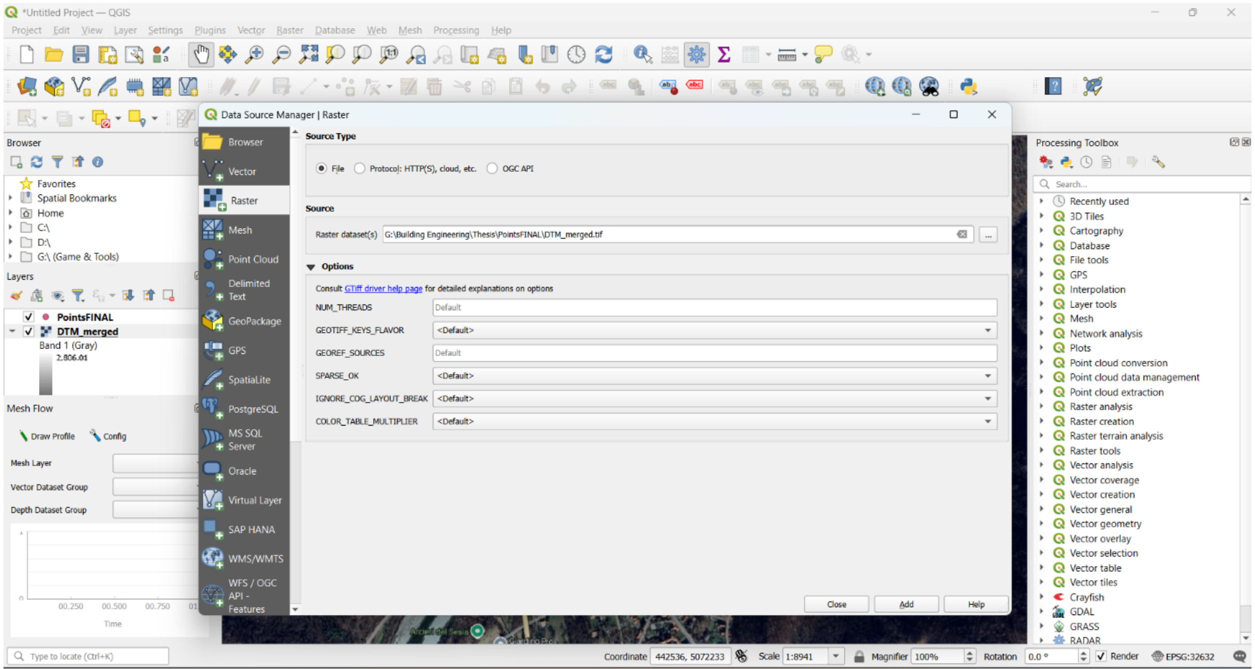

Figure 14. *Importing DTM file to QGIS*

4.2.3) Source Points Definition

The identification and import of **source points** in QGIS represented a fundamental step for defining the potential detachment areas along the Varallo slope. These points indicate where rock blocks are most likely to detach and where the QPROTO analysis begins.

The **source points layer** was provided as a shapefile named PointsFINAL.shp, accompanied by its associated files (.shx, .dbf, .prj, and .cpg).
To load this dataset into QGIS:

1. Open the menu **Layer → Add Layer → Add Vector Layer**
2. In the "Source" panel, browse and select the PointsFINAL.shp file.
3. Ensure that the coordinate reference system (CRS) matches the project CRS — typically **EPSG:4326 (WGS 84)** or the regional CRS used for the DTM.
4. Click **Add** to display the points in the QGIS workspace.

Once imported, the layer appeared as a collection of discrete points located over the slope surface [**Figure 15**. Each point corresponds to a potential **rockfall release location**.

By opening the **Attribute Table** of the layer which is shown in **Figure 16**, it was possible to verify and edit the associated attributes (e.g., ID, SIF value, sector, or volume category). If necessary, new fields could be created to store values such as:

- **SIF index** (Susceptibility Index to Failure) for each point,
- **Rock block volume**,
- **Elevation**
- **Mass**
- **Slope Angle**

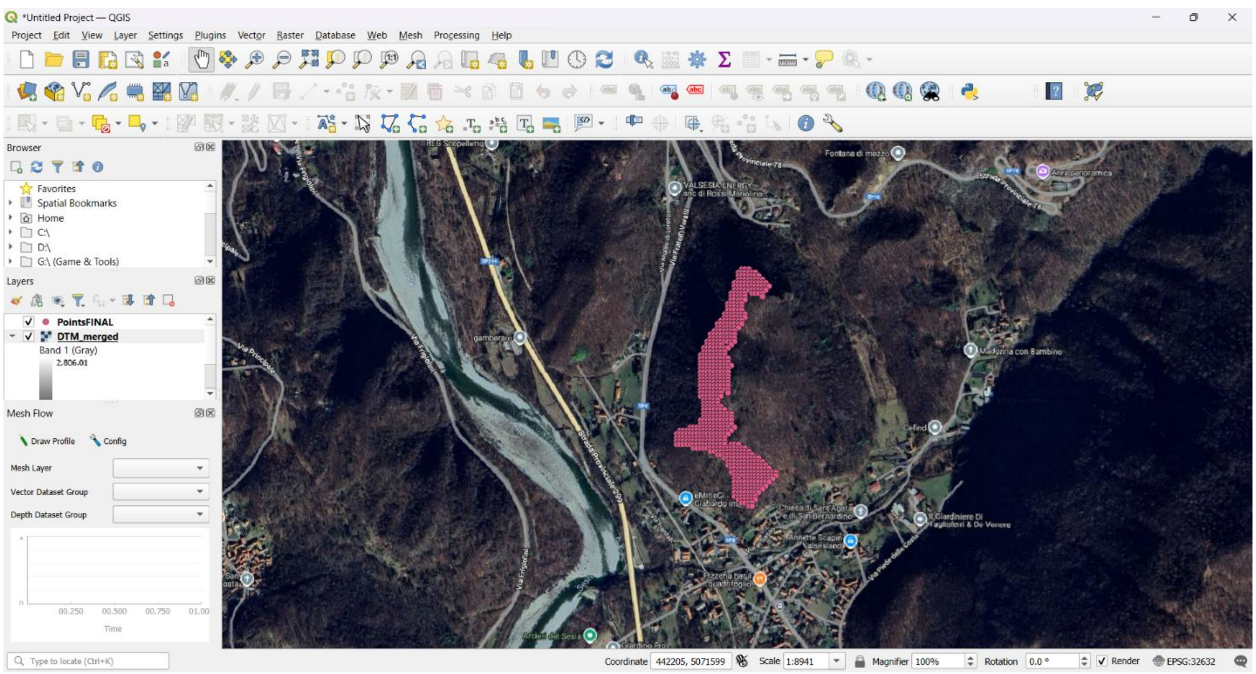

Figure 15. *The case Study DTM with Source Points*

PointsFINAL — Features Total: 627, Filtered: 627, Selected: 0

	fid	id	Pendenza	DTMAspectM	Elevation	Slope Ang	Slope A.F	R.M.S.C	Cond.o.Dis	F.D.O.R.M	Lithology	Exp.R.E	Water	U.B or O.S	Aggr Cond
1	1	52	47.5397529600...	333.875241580...	568.000000000...	48	2.00000000000...	3.00000000000...	1.00000000000...	0	1.00000000000...	0	2.00000000000...	0	0
2	2	53	44.6302871700...	319.534583189...	572.000000000...	45	1.00000000000...	3.00000000000...	1.00000000000...	0	1.00000000000...	0	2.00000000000...	0	0
3	3	54	43.1318473819...	36.2197883449...	569.000000000...	43	1.00000000000...	3.00000000000...	1.00000000000...	0	1.00000000000...	0	2.00000000000...	0	0
4	4	83	39.6398162839...	288.895338229...	569.000000000...	40	1.00000000000...	3.00000000000...	1.00000000000...	0	1.00000000000...	0	2.00000000000...	0	0
5	5	84	42.2726135249...	308.888329119...	577.000000000...	42	1.00000000000...	3.00000000000...	1.00000000000...	0	1.00000000000...	0	2.00000000000...	0	0
6	6	85	38.4540214539...	6.89812517170...	582.000000000...	38	1.00000000000...	3.00000000000...	1.00000000000...	0	1.00000000000...	0	2.00000000000...	0	0
7	7	86	41.8846015929...	41.1498999339...	576.000000000...	42	1.00000000000...	3.00000000000...	1.00000000000...	0	1.00000000000...	0	2.00000000000...	0	0
8	8	87	41.7441902160...	42.7928229839...	571.000000000...	42	1.00000000000...	3.00000000000...	1.00000000000...	0	1.00000000000...	0	2.00000000000...	0	0
9	9	88	41.6154708859...	45.6371089280...	564.000000000...	42	1.00000000000...	3.00000000000...	1.00000000000...	0	1.00000000000...	0	2.00000000000...	0	0
10	10	115	44.7167930600...	286.342356870...	571.000000000...	45	1.00000000000...	3.00000000000...	1.00000000000...	0	1.00000000000...	0	2.00000000000...	0	0
11	11	116	56.5561523439...	305.296737800...	581.000000000...	57	2.00000000000...	3.00000000000...	1.00000000000...	0	1.00000000000...	0	2.00000000000...	0	0
12	12	117	41.6847801210...	13.5104462630...	590.000000000...	42	1.00000000000...	3.00000000000...	1.00000000000...	0	1.00000000000...	0	2.00000000000...	0	0
13	13	118	44.9170494079...	43.0956929500...	583.000000000...	45	1.00000000000...	3.00000000000...	1.00000000000...	0	1.00000000000...	0	2.00000000000...	0	0
14	14	119	41.9446983340...	42.4375308790...	577.000000000...	42	1.00000000000...	3.00000000000...	1.00000000000...	0	1.00000000000...	0	2.00000000000...	0	0
15	15	120	43.4258346559...	44.9376726269...	571.000000000...	43	1.00000000000...	3.00000000000...	1.00000000000...	0	1.00000000000...	0	2.00000000000...	0	0
16	16	121	41.2366867069...	45.3786617130...	564.000000000...	41	1.00000000000...	3.00000000000...	1.00000000000...	0	1.00000000000...	0	2.00000000000...	0	0
17	17	147	62.4229927060...	302.910788700...	577.000000000...	62	2.00000000000...	3.00000000000...	1.00000000000...	0	1.00000000000...	0	2.00000000000...	0	0
18	18	148	62.4392356870...	312.912493040...	594.000000000...	62	2.00000000000...	3.00000000000...	1.00000000000...	0	1.00000000000...	0	2.00000000000...	0	0
19	19	149	44.8437385559...	35.2594922290...	598.000000000...	45	1.00000000000...	3.00000000000...	1.00000000000...	0	1.00000000000...	0	2.00000000000...	0	0
20	20	150	46.7023925780...	45.0913568369...	591.000000000...	[illegible]	...000000000...	3.00000000000...	1.00000000000...	0	1.00000000000...	0	2.00000000000...	0	0
21	21	151	42.0380859380...	44.0564337929...	584.000000000...	42	1.00000000000...	3.00000000000...	1.00000000000...	0	1.00000000000...	0	2.00000000000...	0	0
22	22	152	42.7092971800...	47.8969229400...	577.000000000...	43	1.00000000000...	3.00000000000...	1.00000000000...	0	1.00000000000...	0	2.00000000000...	0	0
23	23	153	42.4048080439...	51.6909030870...	570.000000000...	42	1.00000000000...	3.00000000000...	1.00000000000...	0	1.00000000000...	0	2.00000000000...	0	0

598.000000000000000

Show All Features

Figure 16. *The Attribute Table of Source Points*

4.2.4) QPROTO – Rockfall Runout Simulation and SIF-Weighted Susceptibility

QPROTO implements the **Cone Method** (Jaboyedoff & Labiouse, 2011; Castelli et al., 2021), which provides an empirical yet effective way to estimate the potential propagation of falling blocks starting from predefined source points.

For each source point, QPROTO constructs a *visibility cone* that geometrically represents all DTM cells potentially reachable by a falling block, based on parameters such as:

- **Energy line angle (ϕp):** controls the steepness of the cone and represents the equivalent friction between block and slope.
- **Lateral spreading angle (α):** controls the horizontal spread of trajectories around the central direction.
- **Dip direction (ω):** defines the orientation of the slope at the detachment location.

All DTM cells falling inside this cone are considered part of the **potential runout area**.
By repeating this operation for all source points, QPROTO creates a map of **cumulative visibility** — indicating the number of sources that can reach each cell. [**Figure 17**]
When weighted by the **SIF (Susceptibility Index to Failure)** values, this map becomes a **SIF-**

weighted susceptibility map, which highlights the sectors most likely to generate hazardous rockfall impacts.

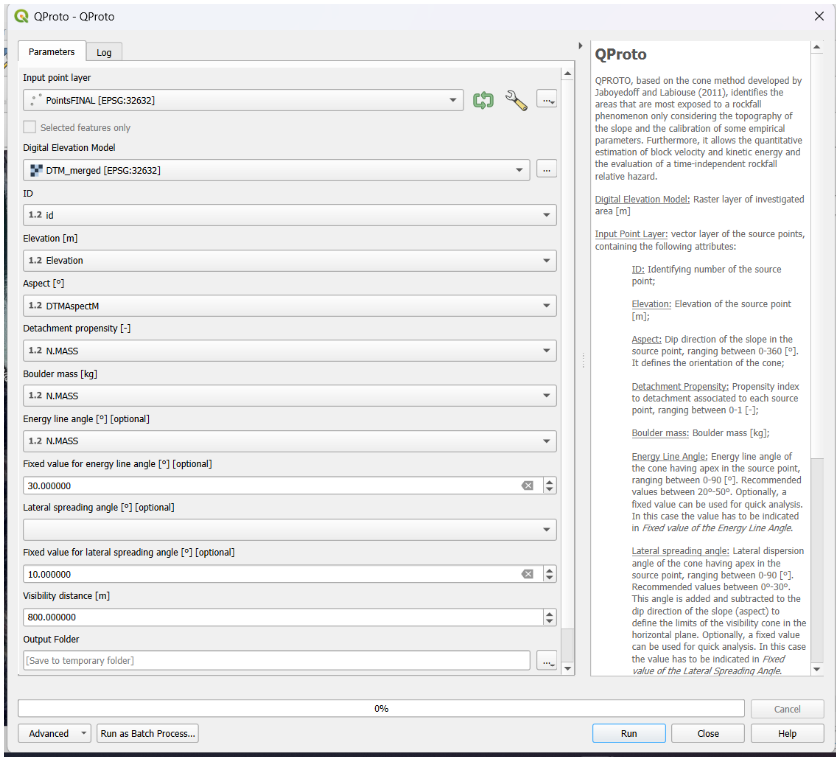

Figure 17. *The QPROTO plugin and data inputting*

The values were calibrated according to the geometry of the Varallo slope and in agreement with previous studies by Napoli et al. (2024–2025).

The main output files exported from QPROTO were:

- The **SIF-weighted susceptibility raster**
- The **final points layer**

4.3) Rocfall 3D Workflow

4.3.1) Overview and Comparison with Rocfall 2D

Rocfall 3D, developed by **Rocscience Inc.**, is an advanced numerical tool designed to simulate the three-dimensional trajectories of falling rock blocks along a digital surface.
Unlike its predecessor **Rocfall 2D**, which performs two-dimensional, cross-sectional analyses, **Rocfall 3D** allows a full spatial representation of rockfall dynamics on complex terrains.

In **Rocfall 2D**, the simulation is limited to a single vertical or inclined profile, meaning that all block trajectories follow a single plane defined by the slope line.
While this approach is useful for preliminary analyses, it neglects the natural **lateral dispersion**, **surface curvature**, and **three-dimensional variability** of real slopes.

In contrast, **Rocfall 3D** integrates:

- a **triangulated 3D surface mesh (from a DTM)**,
- **3D block trajectories** that can deviate laterally,
- and the ability to compute spatial outputs such as **impact energy maps**, **runout envelopes**, and **endpoint distributions**.

This makes Rocfall 3D a far more realistic and comprehensive tool for assessing rockfall hazard.[6]

4.3.2) Preparing Input Data

Before launching any simulation, Rocfall 3D requires that all spatial input files be properly formatted.
In this study, two types of files were prepared:

1. the **terrain surface**, derived from the Digital Terrain Model (DTM), and
2. the **source points**, representing potential detachment locations.

Rocfall 3D requires the terrain model to be imported as one of these Formats:

- RS Geometry Object (*.rsgeomobj) (Rocscience Geometry object file format)
- OBJ Files (*.obj)
- STL Files (*.stl; *.stlbin)
- Autodesk Files (*.dxf; *.dwg)
- STEP Files (*.step)
- IGES Files (*.iges; *.igs)
- TIN Files (*.tin)
- ASC Files (*.asc)
- LAS Files (*.las)
- LUCAS Files (*.mdl)
- SHP Files (*.shp)
- PLY Files (*.ply)
- Deswik DUF Files (*.duf)
- Slide3 Result Object (*.slide3dresobj)
- DTM Files (*.dtm)
- OFF Files (*.off)

Before performing the 3D numerical simulations, the terrain model and source points needed to be properly formatted for compatibility with Rocfall 3D.

Specifically, the Digital Terrain Model (DTM) originally available in GeoTIFF format (.tif) was converted to an **ASCII grid (.asc)**, while the source points provided as a shapefile (.shp) were exported as a **comma-separated table (.csv).**

These conversions were carried out within the QGIS environment to ensure full geospatial consistency between datasets.[6]

The conversion was executed directly in **QGIS**, using the *Translate (Convert format)* function available under the raster conversion tools.
Through this process, the DTM was translated from GeoTIFF to **AAIGrid (.asc)** format while

preserving its original spatial resolution, cell size, and extent.
A *NoData value* of -9999 was assigned to maintain consistency during import into Rocfall 3D. [**Figure 18**]

The resulting **DTM_merged.asc** file represented the final gridded surface of the Varallo slope and was subsequently used by Rocfall 3D to reconstruct the three-dimensional terrain geometry.

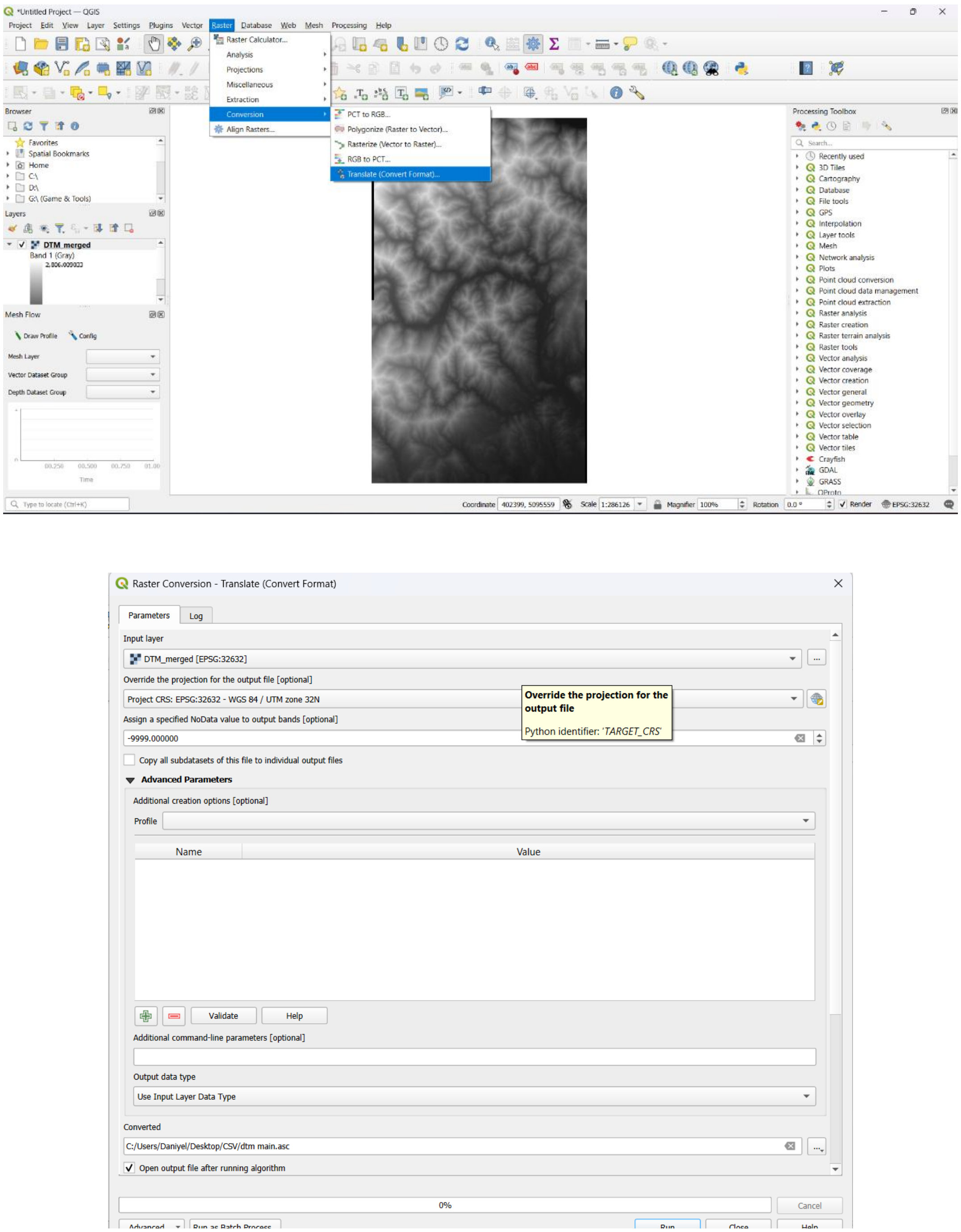

Figure 18. *Converting Geotiff format to ASC*

4.3.3) Reduction of the DTM Extent for the Varallo Domain

The original *DTM_merged.asc* file covered a considerably large portion of the Sesia Valley, extending far beyond the actual rockfall area of interest.
When imported into **Rocfall 3D**, this large dataset resulted in excessive rendering time and computational load, making the visualization and simulation process extremely slow and inefficient.

To overcome this limitation, the **DTM extent was reduced** to include only the area surrounding the **Varallo slope**, where the 2023 rockfall event occurred.
This refinement allowed the model to focus exclusively on the relevant geomorphological features while significantly improving processing performance and rendering speed within Rocfall 3D.

The reduction of the DTM was carried out within **QGIS** prior to the conversion to ASCII format. Specifically, the **Clip Raster by Extent** tool (from *Raster → Extraction → Clip Raster by Extent, [***Figure 19***]*) was used to delimit the boundaries of the analysis domain.
The extent coordinates were manually set to encompass only the Varallo study area.
Alternatively, the **Select by Polygon** option was also tested to visually crop the DTM based on a user-defined boundary around the slope.

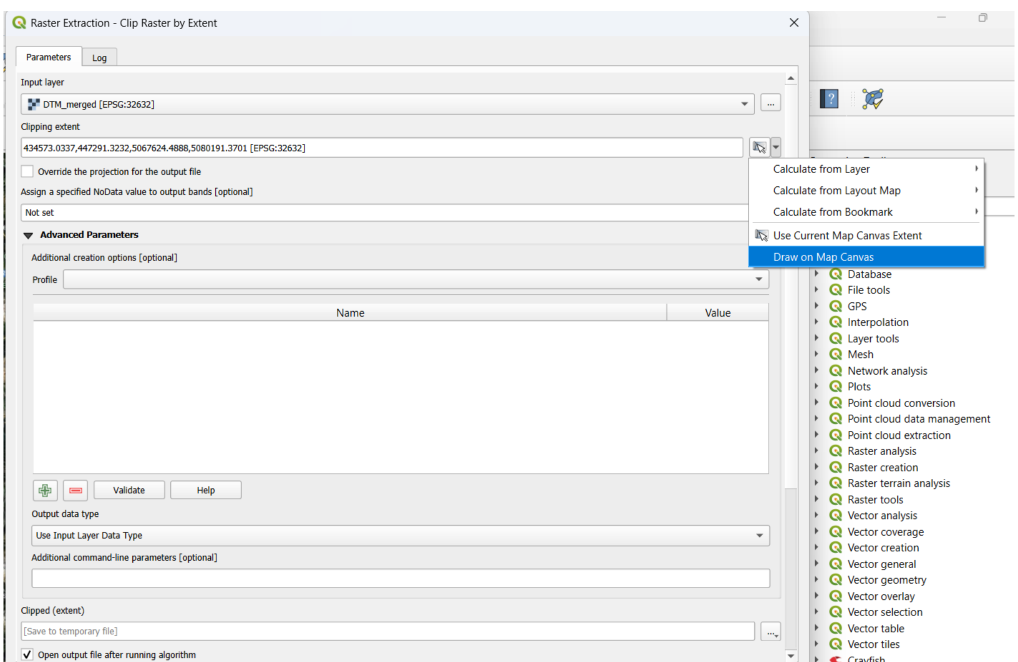

Figure 19. *DTM extension phase by QGIS*

4.3.4) Conversion of Source Points

In addition to optimizing the terrain model, the **source point dataset** also required specific formatting adjustments to ensure correct import and coordinate recognition in **Rocfall 3D**.
The original vector layer (*PointsFINAL.shp*) contained accurate planimetric coordinates (X, Y) but did not include the **elevation (Z)** values in a format directly readable by Rocfall 3D.
When the shapefile was tested for import, the software was unable to correctly interpret the altitude data, resulting in misplaced or flattened release points on the surface.

To solve this issue, all source points were exported from **QGIS** as a **comma-separated file in CSV format**. [**Figure 20**
During this conversion, the *Add geometry attributes* function was first used to attach the elevation (Z) extracted from the DTM to each point.
The updated layer was then saved as a **CSV file** containing three columns — *X*, *Y*, and *Z* — representing the full three-dimensional position of each potential release location.

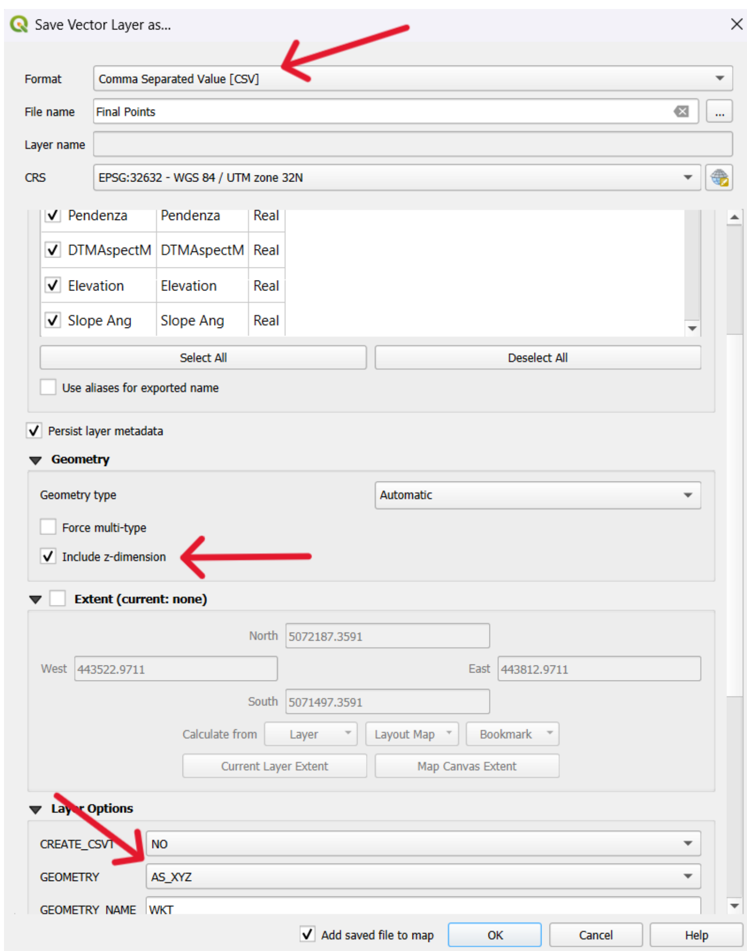

Figure 20. *Converting Source Point to CSV format*

4.3.5) Importing the Terrain and Source Data into Rocfall 3D

After the DTM preprocessing in QGIS, the reduced and optimized terrain file (*DTM_Varallo.asc*) was imported into **Rocfall 3D** to generate the three-dimensional slope surface.

There are two possible methods for importing the terrain into the software.
The first method consists of importing the terrain using its **exact georeferenced coordinates**, which preserves the original spatial position and alignment of the model with real-world data.[6]

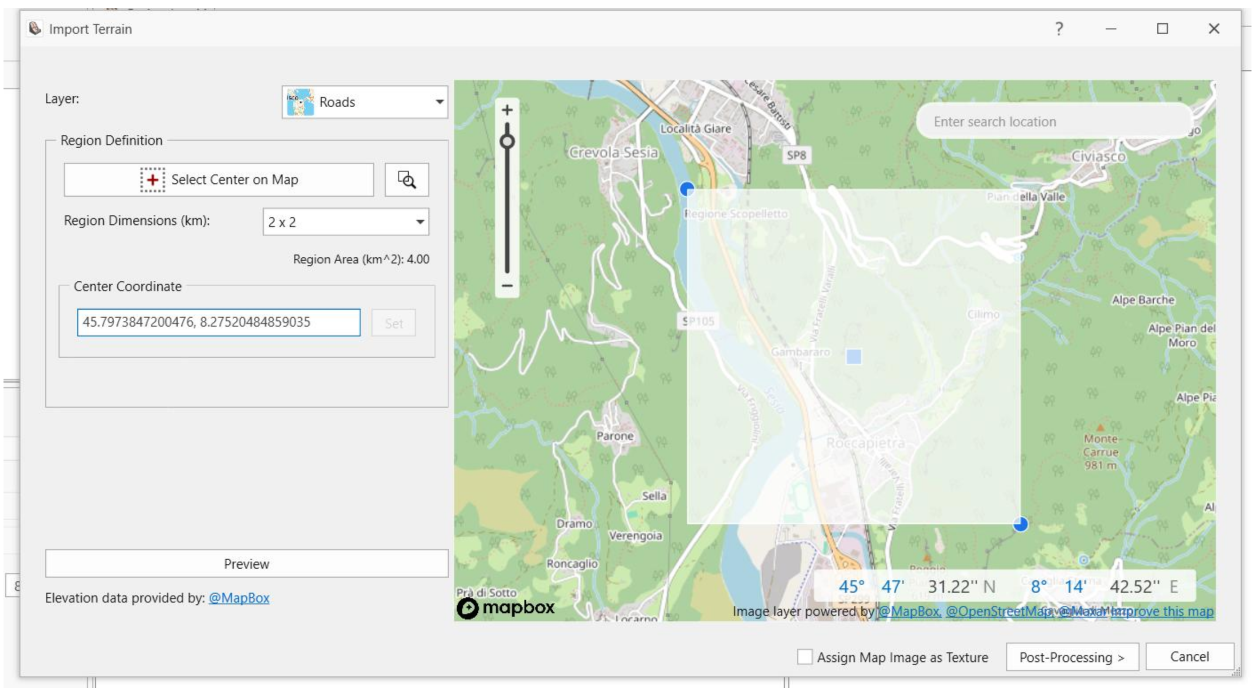

Figure 21. *Import Terrain in Rocfall 3D*

But in this case study import was carried out using the:

*Geometry → Surface Triangulation Tools → Add Surface From Points [***Figure 22**

Once loaded, the program automatically created a **triangulated surface mesh** based on the elevation values contained in the ASCII grid.

During this stage, several mesh-quality checks were performed to ensure that the geometry was consistent with the real morphology of the Varallo slope.[6]

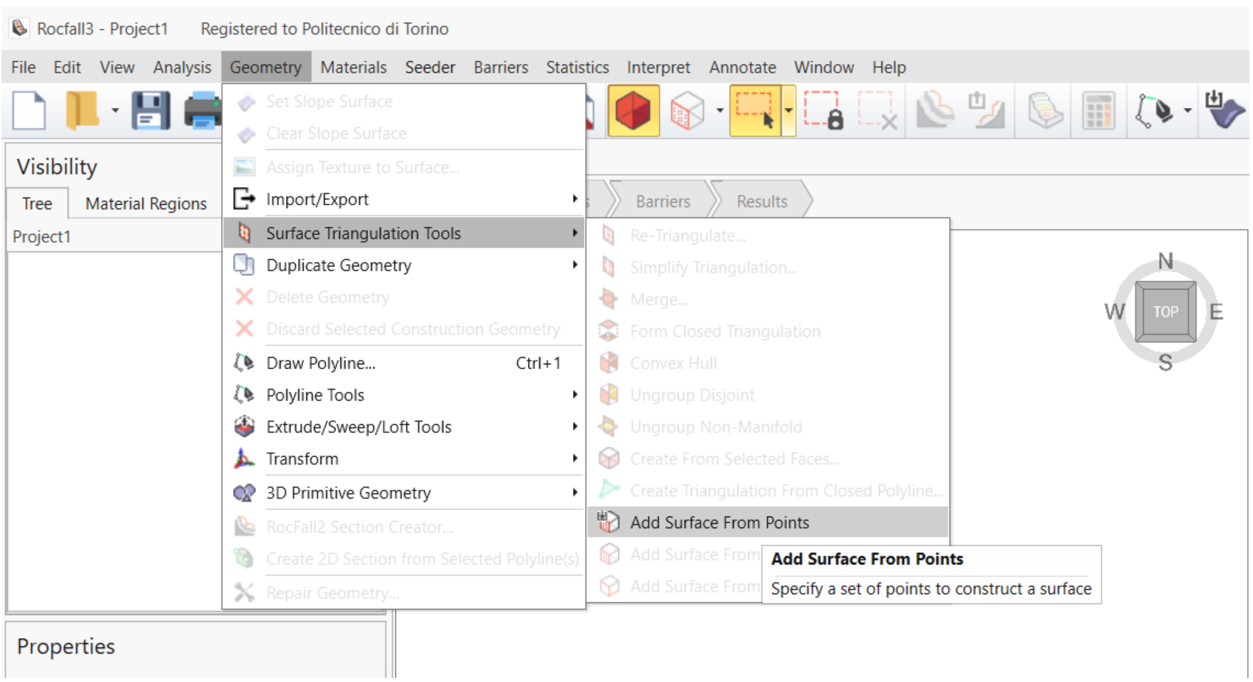

Figure 22. *Importing DTM inro Rocfall 3D*

After importing has been completed we can see all the points with their data.

Once the 3D surface was correctly generated, the **release points** were imported using the previously prepared file *PointsFINAL_XYZ.csv*.
This file contained the full three-dimensional coordinates (X, Y, Z) of each source location, allowing each block to be initialized exactly on the slope surface at its true elevation. [**Figure 23**]

The import was completed through the same way as DTM, selecting the corresponding coordinate columns and matching the project coordinate system. [**Figure 24**
Each imported point appeared as a small marker on the 3D mesh, confirming the correct georeferencing of all sources.[6]

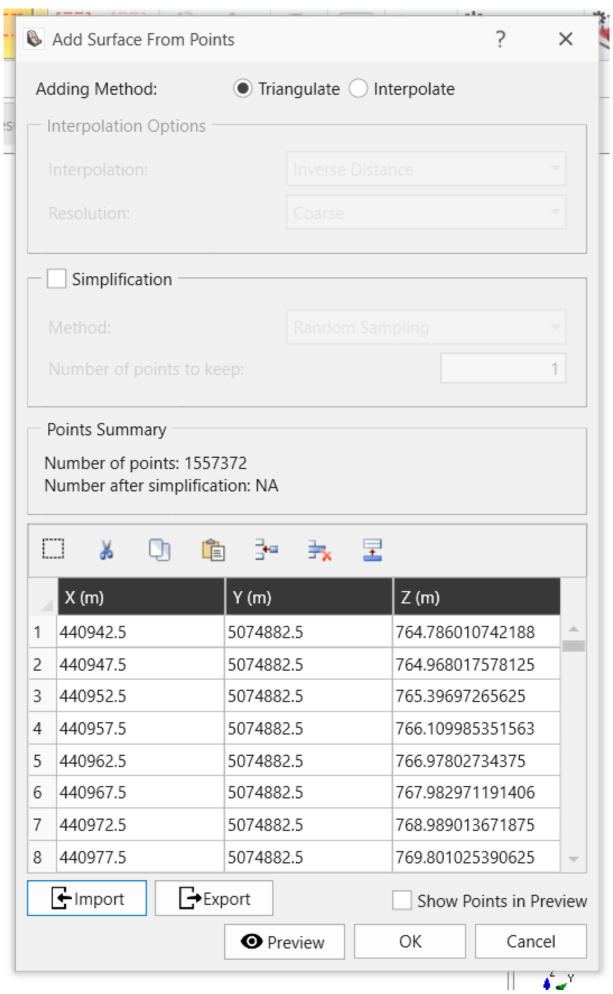

Figure 24. *DTM data on Rocfall 3D*

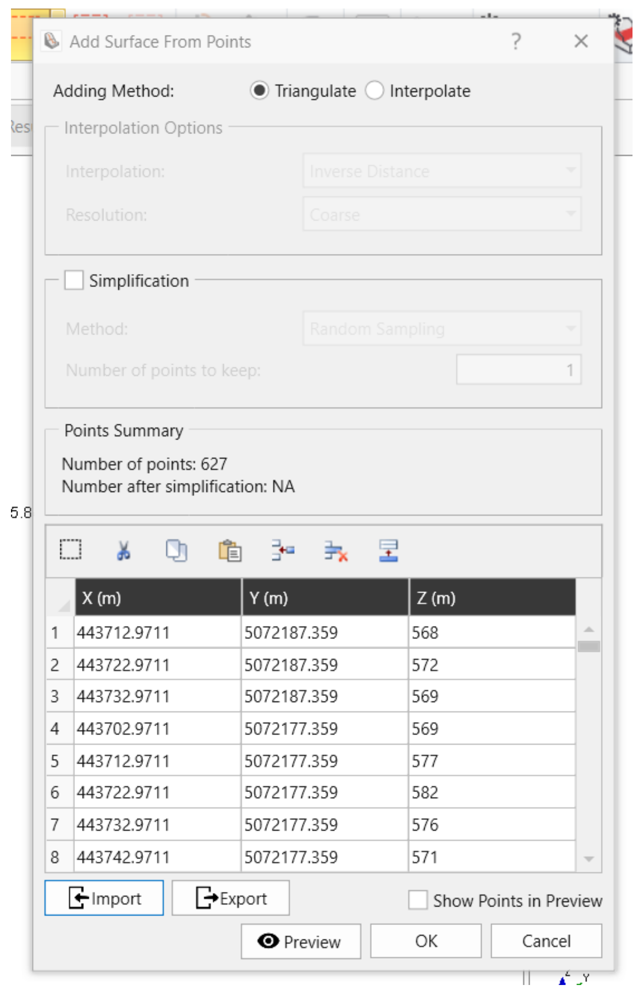

Figure 23*. Source Points data on Rocfall 3D*

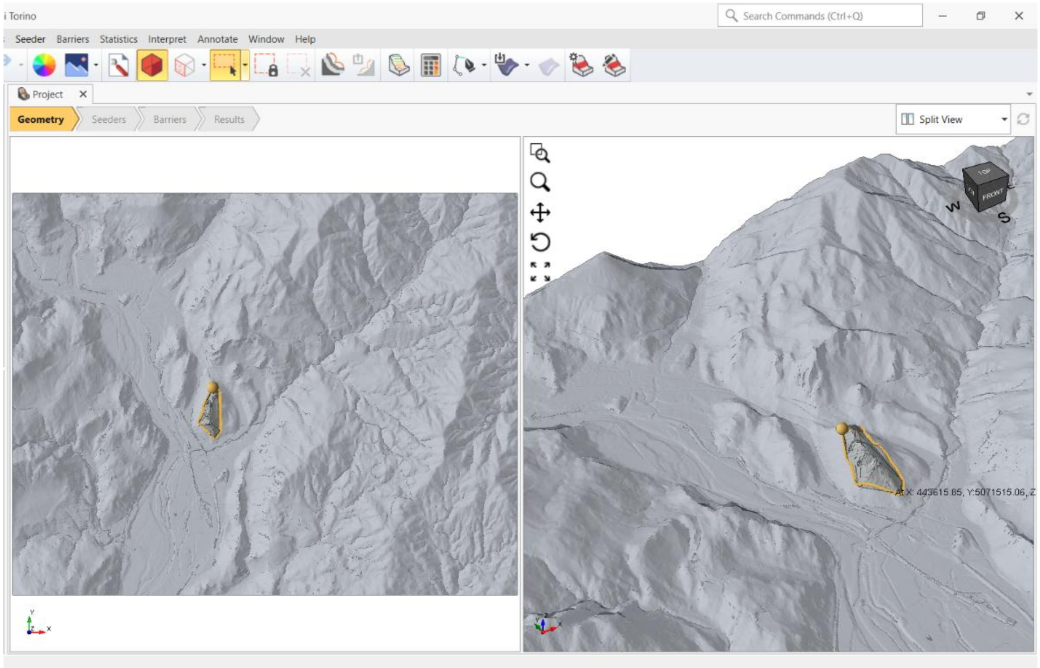

***Figure 25**. Total view of the site after importing data*

After importing, the reconstructed mesh was explicitly **declared as the active slope surface** in the model. This assignment ensures that **all contact, impact, and rolling calculations** are performed with respect to the same ground geometry used to derive the seeders' elevations, avoiding inconsistencies where blocks might otherwise "see" a default or inactive surface.

In practice, the imported terrain mesh was set as the **primary ground/slope surface** for the analysis; no auxiliary meshes, or temporary scaffolds were left active.

For setting the surface is main slope we selected **set slope** from Geometry.[6]

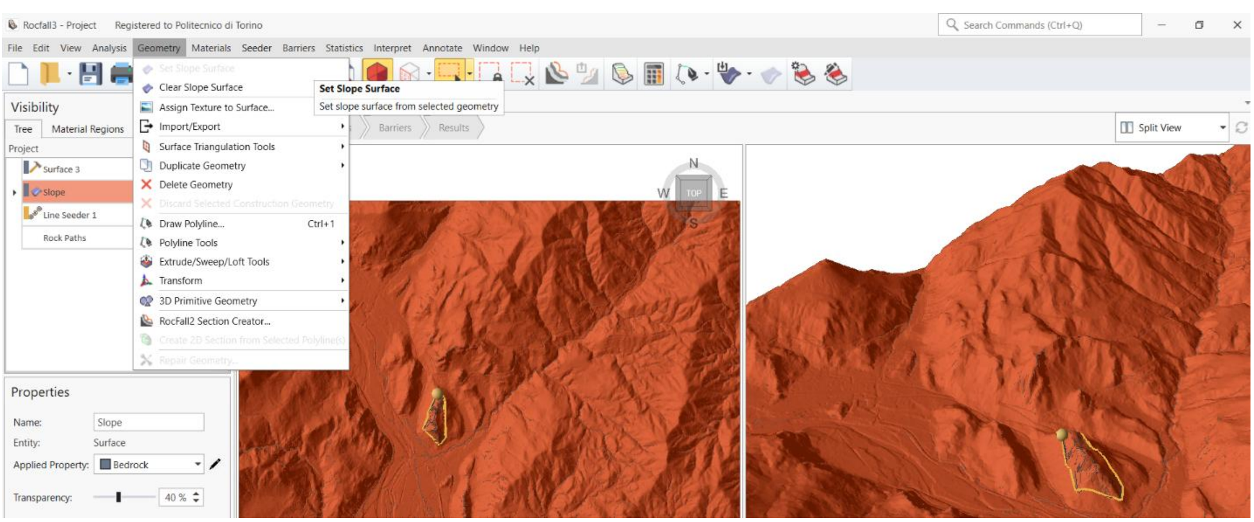

4.3.6) Definition of Rock Block Properties

After successfully importing the terrain and source datasets, the physical and mechanical parameters of the falling rock blocks were defined.
The properties were selected to represent **kinzigite boulders**, consistent with the lithology of the Varallo slope.

The mechanical and physical parameters adopted for the simulated rock blocks are summarized in **Table 1**, representing the typical properties of kinzigite boulders observed at the Varallo slope.

Column1	Column2	Column3	Column4
Parameter	**Symbol / Unit**	**Value**	**Description**
Block density	ρ (kN/m^3)	27	Derived from field data and literature for kinzigite
Block volume	V (m^3)	5.4	Design volume corresponding to a 25-year return period
Coefficient of normal restitution	Rn	0.40 – 0.55	Defines rebound energy loss upon impact
Coefficient of tangential restitution	Rt	0.80 – 0.95	Governs sliding and rolling behavior
Surface friction angle	ϕ (°)	30 – 40	Estimated from slope roughness and field inspection
Damping ratio	ξ	0.1 – 0.12	Energy dissipation factor during impacts

***Table 1**.The mechanical and physical parameters*

The statistical distributions assigned to the mechanical parameters of the simulated blocks are shown in **Figure 26**, where normal and tangential restitution coefficients, as well as the surface friction angle, were defined using normal distributions to account for natural variability in block–terrain interactions.

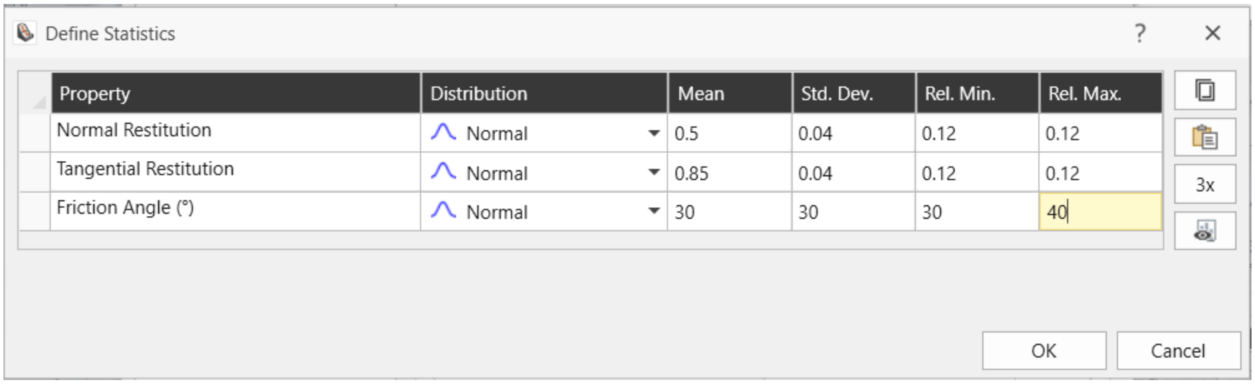

Property	Distribution	Mean	Std. Dev.	Rel. Min.	Rel. Max.
Normal Restitution	Normal	0.5	0.04	0.12	0.12
Tangential Restitution	Normal	0.85	0.04	0.12	0.12
Friction Angle (°)	Normal	30	30	30	40

Figure 26. *The statistical distributions assigned to the mechanical parameters in Rocfall 3D*

According to the geological characteristics of the Varallo slope, the simulated blocks were modeled as **kinzigite boulders**, consistent with the lithology observed in the field.
The **design block volume** was defined as **5.4 m^3**, which represents the typical block size estimated from the field survey and from the results of the QPROTO analysis.

Based on published physical data for kinzigitic paragneisses, the **material density** was set to **2,600 kg/m^3**.
This value was introduced into the Block Properties window of **Rocfall 3D [Figure 27]**, and the corresponding block mass was automatically computed using the relation:[5]

$$m = \rho \times V$$

Substituting the adopted parameters:

$$m = 2{,}600\ \text{kg/m}^3 \times 5.4\ \text{m}^3 = 14{,}040\ \text{kg}.$$

Thus, each simulated block had a total mass of **approximately 14.0 tons**, which represents a realistic estimate for the detached rock fragments observed at the Varallo site.
These values ensured that the model reproduced the correct inertial and kinetic behavior of the falling blocks, providing physically consistent results in terms of trajectory, impact energy, and runout distance.[1]

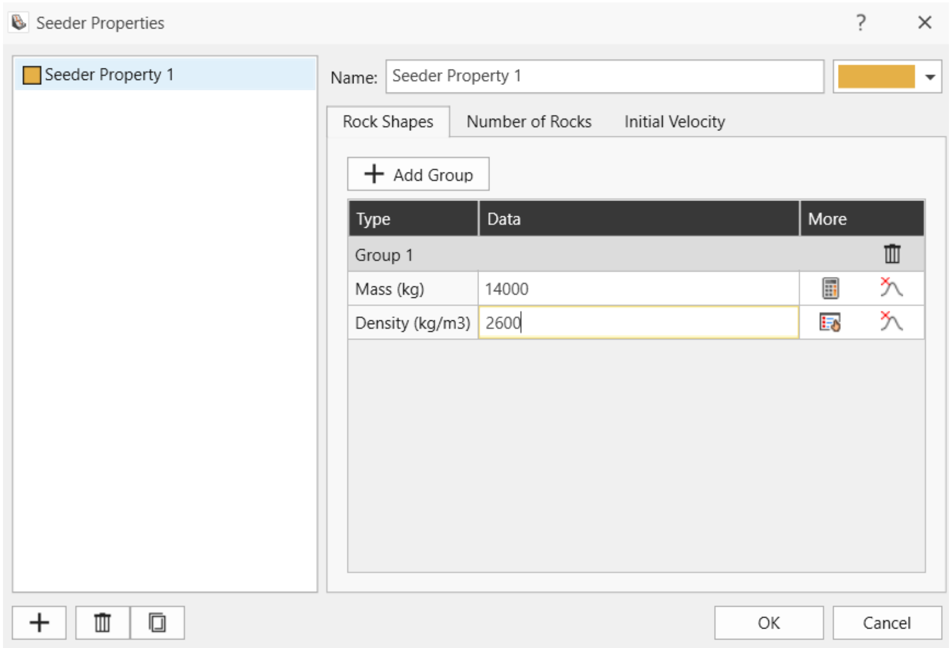

***Figure 27**. Seeders Properties on Rocfall 3D based on calculation*

4.3.7) Importing Seeders on Rocfall 3D

In Rocfall 3D, a **seeder** is a release entity that defines *where* blocks start and *how many* realizations are generated at that location (including any statistical perturbations on direction/speed). Each seeder sits on the terrain surface and "spawns" a user-specified number of blocks that inherit the global block properties above.[6]

What a seeder controls.

- **Spatial location:** 3D coordinates (X, Y, Z)on the mesh (must coincide with the terrain to avoid floating or buried starts).
- **Multiplicity:** number of blocks emitted per seeder (we used 50 per point to build stable envelopes).
- **Direction rule:** by default, along local steepest descent; optional angular jitter can be added for variability.
- **Timing:** simultaneous release (single burst) for envelope mapping; staged release is also possible but not required here.

4.3.8) Importing Seeders on Rocfall 3D

In **Rocfall 3D**, seeders can be introduced into the model through three different methods, depending on how the release zones are represented:

1. **Point Seeder:** individual coordinates are specified for each detachment point.
2. **Line Seeder:** a continuous line is drawn along the crest or face of the slope, and blocks are released at regular intervals along that line.
3. **Area Seeder:** a polygonal surface is defined on the slope, and seeders are automatically distributed inside that area according to the user-selected density.

All three options allow the definition of initial block positions and directions of release, but they differ in how the sources are spatially generated.[6]

During the Varallo analysis, both the **line** and **area seeder** methods were initially tested in order to reproduce the geometry of the most unstable sectors observed in the QPROTO susceptibility map.
However, the results obtained from these automated methods were not satisfactory:

- The line seeder tended to place blocks too uniformly along the ridge, without matching the actual detachment locations observed in the field.
- The area seeder generated release points outside the critical zones and produced unrealistic cluster patterns on the surface.

Because of these limitations, the final configuration was created using **manually defined point seeders**.
For this purpose, the exact **X, Y, and Z coordinates** of each potential release point—previously exported from QGIS as *PointsFINAL_XYZ.csv*—were entered directly into Rocfall 3D using the *Add Seeder* function.[**Figure 28**]

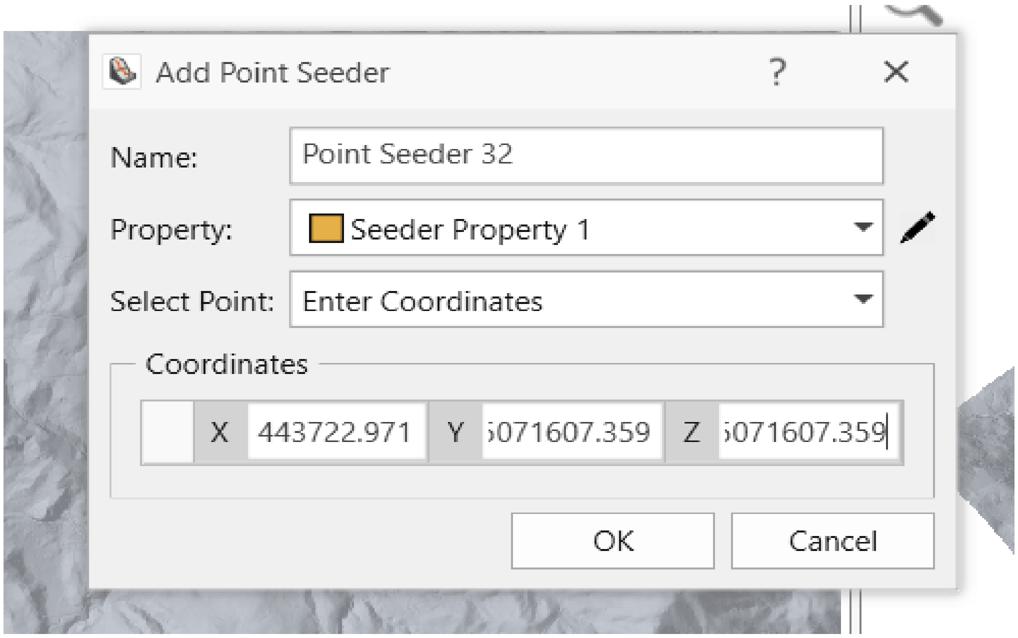

Figure 28. *Adding Points Coordinates manually*

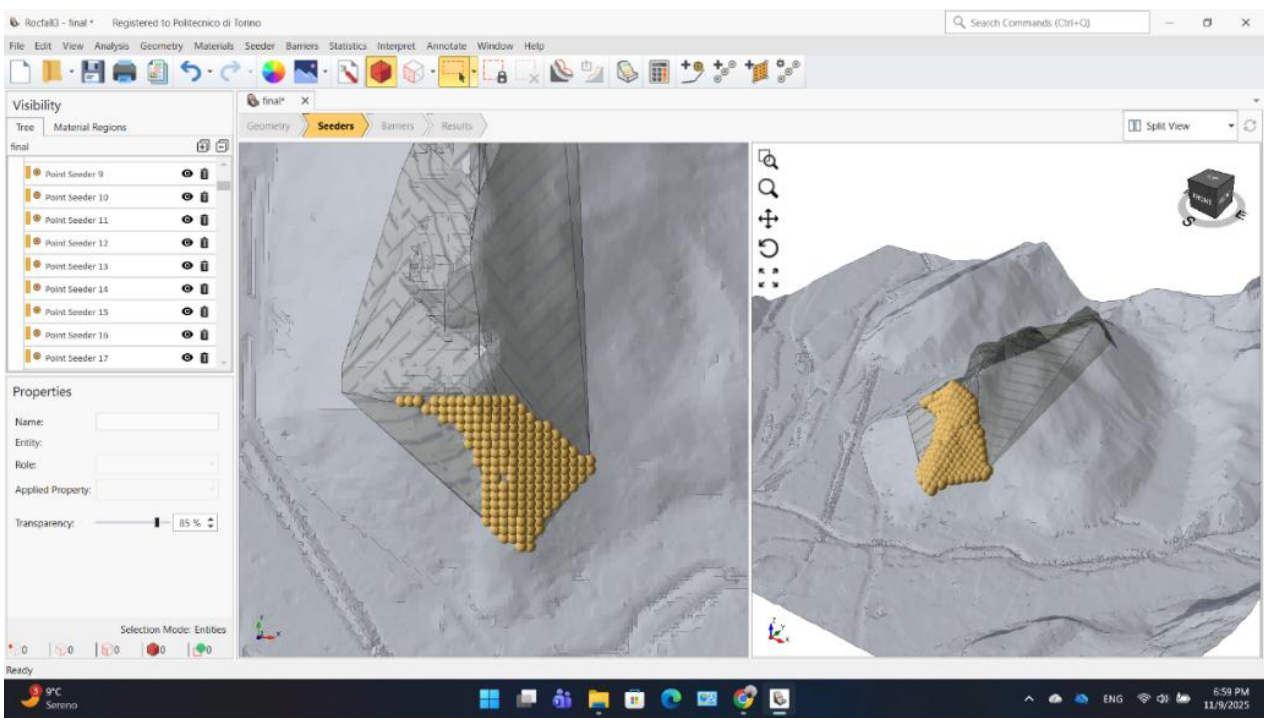

Figure 29*. Adding Point seeders of study area*

5. Results and Discussion

5.1) General Overview

The comparison between the results obtained with **Rocfall 3D**, **Rockyfor3D** (developed under the guidance of ***Dr. G. Cavagnino***)[10][11], and the GIS-based analyses in **QGIS** provides a coherent understanding of rockfall dynamics along the Varallo slope.
Despite the different modeling approaches, all three methods produced comparable **trajectory patterns**, **energy distributions**, and **impact zones**, confirming the reliability of the adopted geometric and mechanical parameters.

The following sections present a focused discussion of three key indicators that best describe the destructive potential of rockfall events: **translational velocity**, **kinetic energy**, and **SIF**. These parameters allow a direct comparison between the GIS-based susceptibility assessment and physically simulated block behavior.

5.2) SIF Calculation and Comparison

All the SIF values used in this study refer **exclusively to the southern sector of the slope**, which is the most unstable portion of the site and the area where the November 2023 rockfall occurred. Both the QGIS-based analysis and the Rocfall 3D simulations were therefore restricted to this zone to ensure consistency between the susceptibility assessment and the physical propagation models.

The **QPROTO** workflow provides SIF values directly through the SIF-weighted susceptibility map, allowing the identification of the sectors with the highest detachment propensity. However, **Rocfall 3D does not compute SIF**, as the software is purely a kinematic simulator and does not include a susceptibility module. For this reason, and in order to perform a homogeneous comparison, the SIF values associated with the Rocfall 3D source points were **manually computed** using the normalization formula introduced in Section 2 of this thesis. The numerical outputs extracted from the Rocfall 3D simulations are shown in [**Figure 30]**, summarizing the maximum kinetic energy, translational velocity, runout distances and the computed SIF values for each source point in the southern sector.

By applying the SIF formulation to the set of factors evaluated for the southern source points (Tables A and B1), the resulting **average SIF value is 0.67**. This value is in excellent agreement with the reference data reported in previous studies on the Varallo slope, where the SIF for the southern sector was quantified as approximately **0.70** [1]

	A	D	E	F	G	H	I	J	M	N	O	P
1	ID	Stopping Reason	Max Kinetic Energy [kJ]	Max Translational Velocity [m/s]	Runout Distance (XY) [m]	Runout Distance (Total) [ı	Events	sif	SIF-average			
2	0	Stopped	6761.97	27.35	196.54	243.38	182	1.963648	0.660212016			
3	1	Stopped	28.92	1.85	0.51	0.86	8	0.0117				
4	2	Stopped	35.65	1.98	0.78	1.27	10	0.015253				
5	3	Stopped	1382.21	12.67	153.92	202.14	284	1.196787				
6	4	Stopped	25.61	1.73	0.51	0.85	8	0.010711				
7	5	Stopped	33.6	1.93	0.8	1.31	11	0.014824				
8	6	Stopped	24.78	1.7	0.25	0.45	5	0.008889				

Figure 30. *Points Data Exported from Rocfall 3D*

The spatial distribution of SIF-weighted susceptibility derived from the QGIS analysis is presented in[**Figure 31**], highlighting the sectors where the combination of high detachment propensity and favorable runout conditions produces the greatest rockfall hazard.

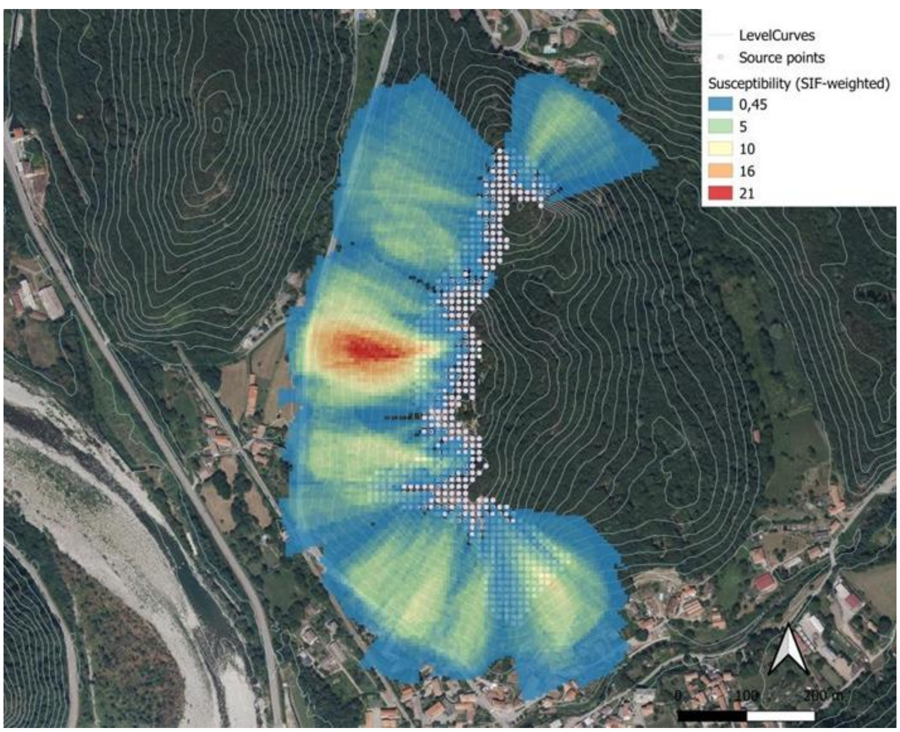

Figure 31*. SIF-weighted runout frequency (or susceptibility) map in QGIS [1]*

Also The two-dimensional and three-dimensional trajectories generated by Rocfall 3D are shown in [**Figure 32**] and [**Figure 33**] , highlighting the propagation paths of the simulated blocks across the southern sector of the Varallo slope. The visualization on the 3D terrain model clearly illustrates the concentration of runout directions toward the valley floor and the areas most exposed to potential impacts.

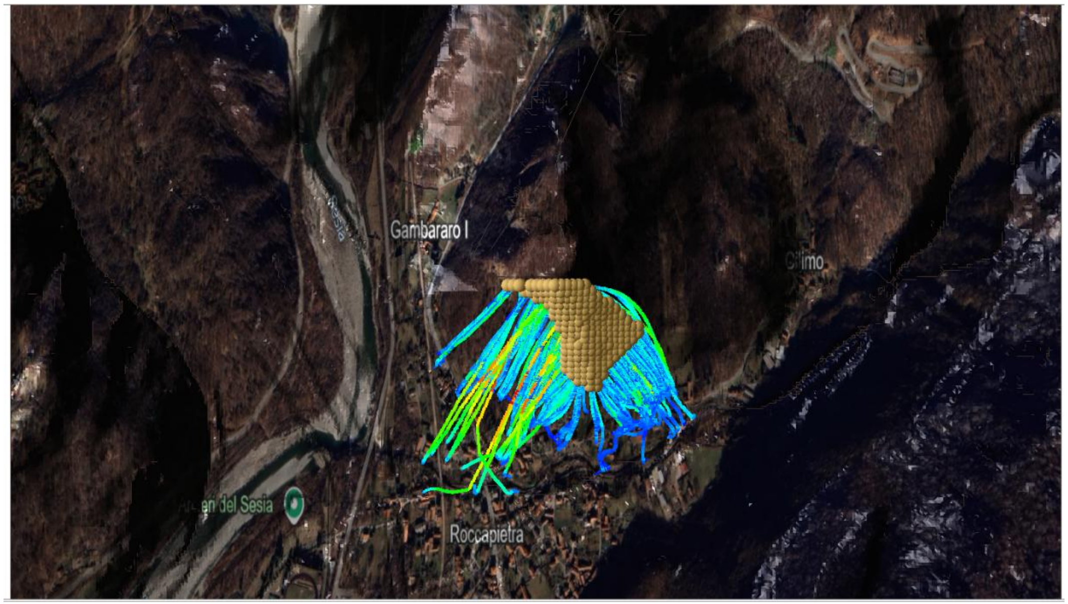

Figure 32*.Two-Dimensional block path in Rocfall 3D*

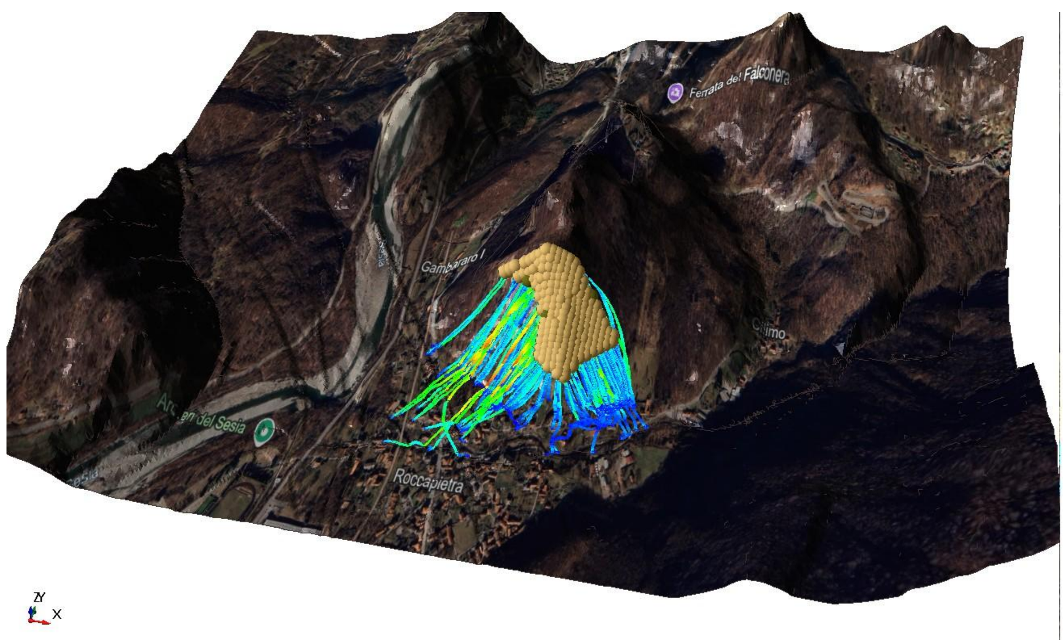

Figure 33*. Three-Dimensional block path in Rocfall 3D*

5.3) Comparison of Kinetic Energy Results

The comparison of translational kinetic-energy results across Rockfall 2D, Rocfall 3D, and Rockyfor3D highlights how both the block volume and model dimensionality influence energy propagation.

The **Rockfall 2D back-analysis**, carried out using a block volume of **3.0–3.25 m^3** (corresponding to the November 2023 event), produced a maximum kinetic energy of **≈ 2.18 MJ**, which represent the critical part of the slope.
These values derive from the design-energy envelopes provided in the 2D simulation outputs, where the vertical fall path and single-plane dynamics result in greater energy dissipation and therefore lower KE values overall.[8]

In contrast, the **Rocfall 3D** simulation was performed using a larger and more representative **design block volume of 5.4 m^3**, consistent with the statistical volume estimation defined for the Varallo slope. With this volume, Rocfall 3D yielded substantially higher kinetic energies, with maximum values reaching about **3.6 MJ** along the steep upper sector of the slope. In **Figure 36** all these data were highlighted.
The 3D modelling framework captures full terrain morphology, multi-directional motion, and more realistic impact behaviors, allowing the blocks to retain a larger fraction of their mechanical energy.

Similarly, **Rockyfor3D** was run using the same **5.4 m^3 block volume** (Tavola 4). The resulting 95th-percentile kinetic-energy values (**≈ 3.0–3.5 MJ**) closely match those of Rocfall 3D and identify the same high-energy corridor oriented toward the southwestern sector of the slope.[11]

Overall, the two 3D models (Rocfall 3D and Rockyfor3D) display **excellent agreement** in both the magnitude and spatial distribution of kinetic-energy peaks, confirming that the parameters used in Rocfall 3D are properly calibrated.
The lower energies obtained in **Rockfall 2D (~2.18 MJ)** are fully consistent with:

1. the smaller block volume used (≈3.25 m^3), and
2. the inherent geometric simplifications of 2D trajectory modelling.

This comparison demonstrates that the 5.4 m^3 simulations in both Rocfall 3D and Rockyfor3D provide a reliable representation of future detachment scenarios, while Rockfall 2D remains consistent with the documented 2023 back-analysis.
The 95th-percentile translational kinetic-energy distribution obtained from the Rocfall 3D simulation is shown in **[Figure 37]**, illustrating the spatial concentration of high-energy impacts along the southwestern sector of the Varallo slope.

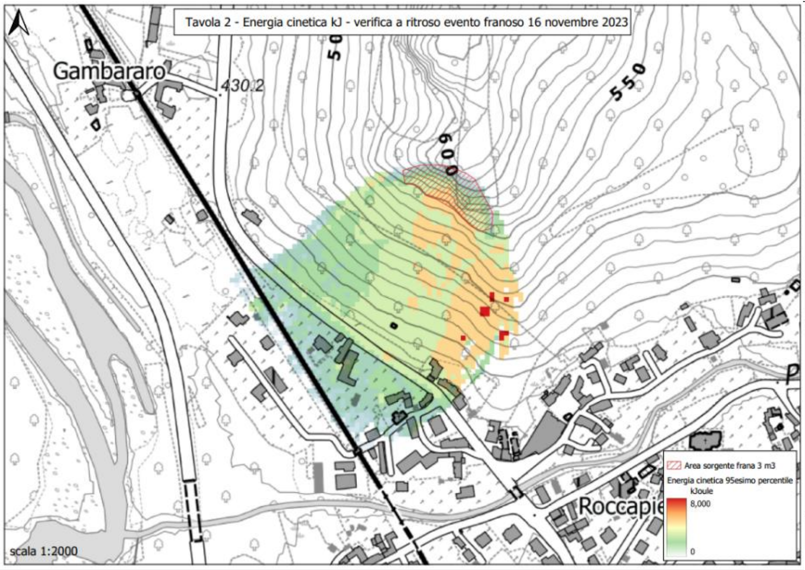

Figure 34.*"Energia cinetica kJ – analisi scendimenti potenziali volume 5,4 m^3"[10]*

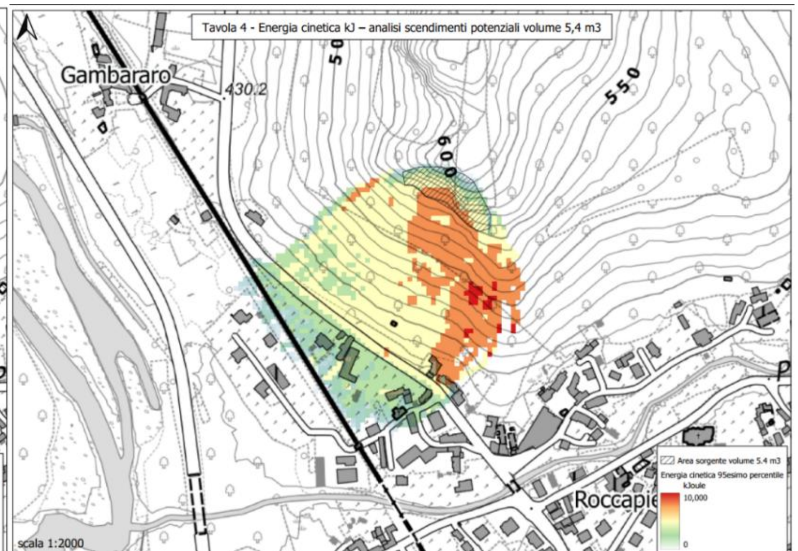

Figure 35. *"Energia cinetica kJ – verifica a ritroso evento franoso 16 novembre 2023"[11]*

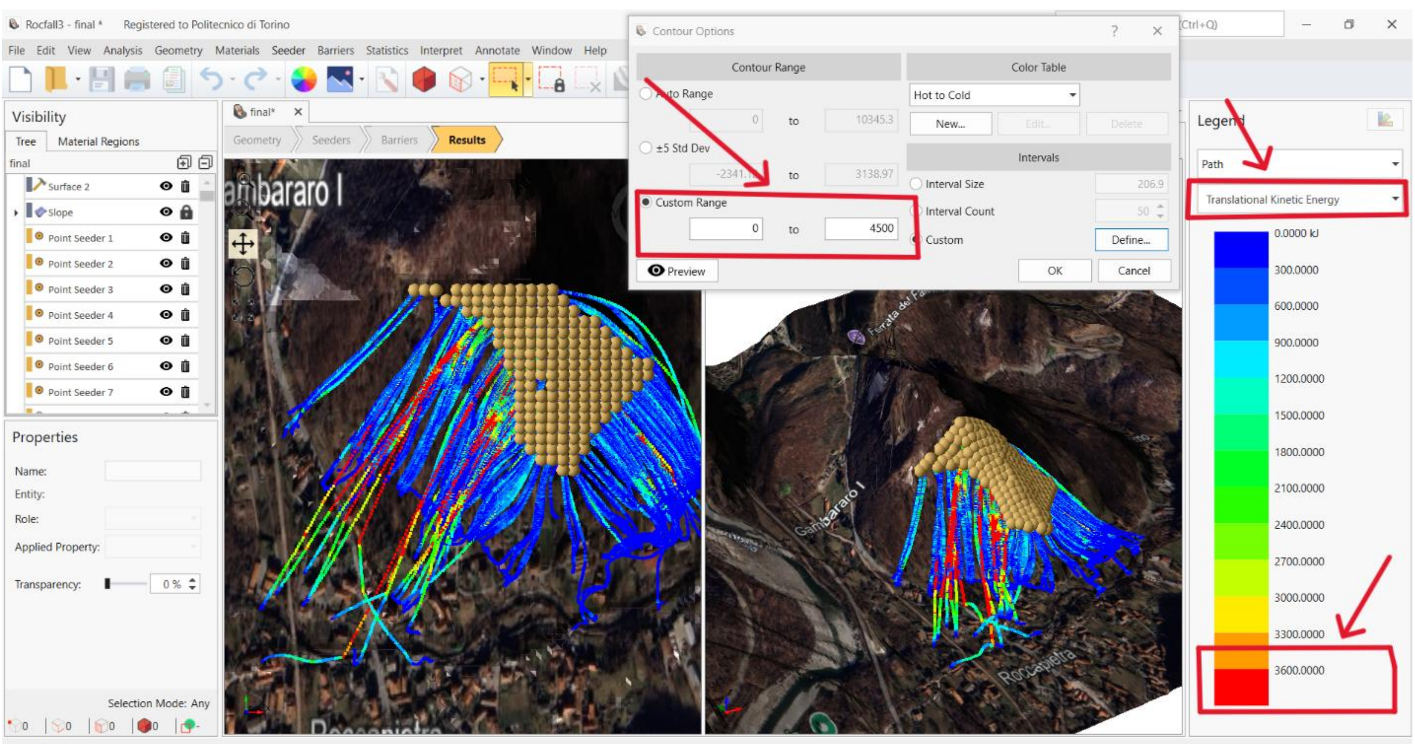

Figure 36. *Translational Kinetic Energy Volume in Rocfall 3D*

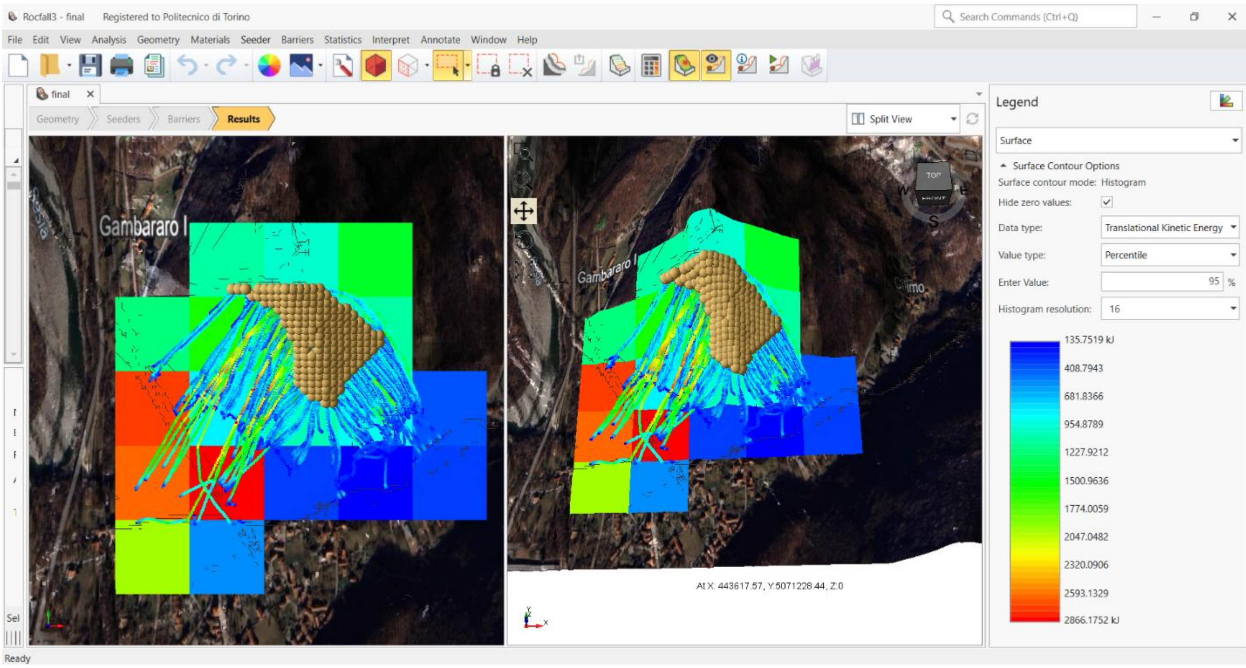

Figure 37. *The 95th-percentile translational kinetic-energy distribution*

5.4) Translational Velocity Results

The analysis of translational velocity further clarifies the dynamic behaviour of the blocks and complements the comparison previously carried out on kinetic energy.
In the **Rocfall 2D** back-analysis, performed on five sections of the slope using three design block volumes (4.20 m^3, 3.25 m^3 and 2.10 m^3), the 95th-percentile translational velocity does not vary significantly with block volume. The maximum value is obtained with a peak velocity of approximately **25.37 m/s**, These results are consistent with the 2D geometric constraint, where motion is confined to a single profile and lateral dispersion is not represented.[8]

The **Rocfall 3D** simulations, carried out with a larger and more representative **design block volume of 5.4 m^3**, indicate higher velocities. The maximum translational velocity reaches **30–31 m/s** (≈108 km/h) along the steepest part of the southern sector, decreasing below **5 m/s** near the foot of the slope . The distribution of velocity closely mirrors the kinetic-energy pattern, with the highest speeds concentrated in the central flow corridor that directs blocks towards the provincial road.

For **Rockyfor3D**, the available Tables mainly report the spatial distribution of kinetic energy for the same **5.4 m^3** design block, rather than explicit velocity maps. However, the location of the highest-energy cells coincides with the same southwestern corridor identified by Rocfall 3D, indicating a comparable dynamic behavior: the zones where Rockyfor3D predicts the highest impact energies correspond to the areas where Rocfall 3D records its maximum translational velocities.[11][10]

Overall, the comparison shows that:

- **Rocfall 2D** (3.25 m^3) predicts peak velocities up to **≈26 m/s**,
- **Rocfall 3D** (5.4 m^3) increases the peak to **≈30m/s** as shown in [**Figure 38**]
- **Rockyfor3D** (5.4 m^3) identifies the same high-velocity/high-energy corridor, even if velocity is inferred indirectly from energy maps.

The higher velocities in the 3D models are consistent with both the **larger block volume** adopted (5.4 m^3 vs. 3.25 m^3 in 2D) and the **more realistic three-dimensional representation** of the slope, which allows blocks to follow the steepest descent paths and maintain higher speeds over longer distances.

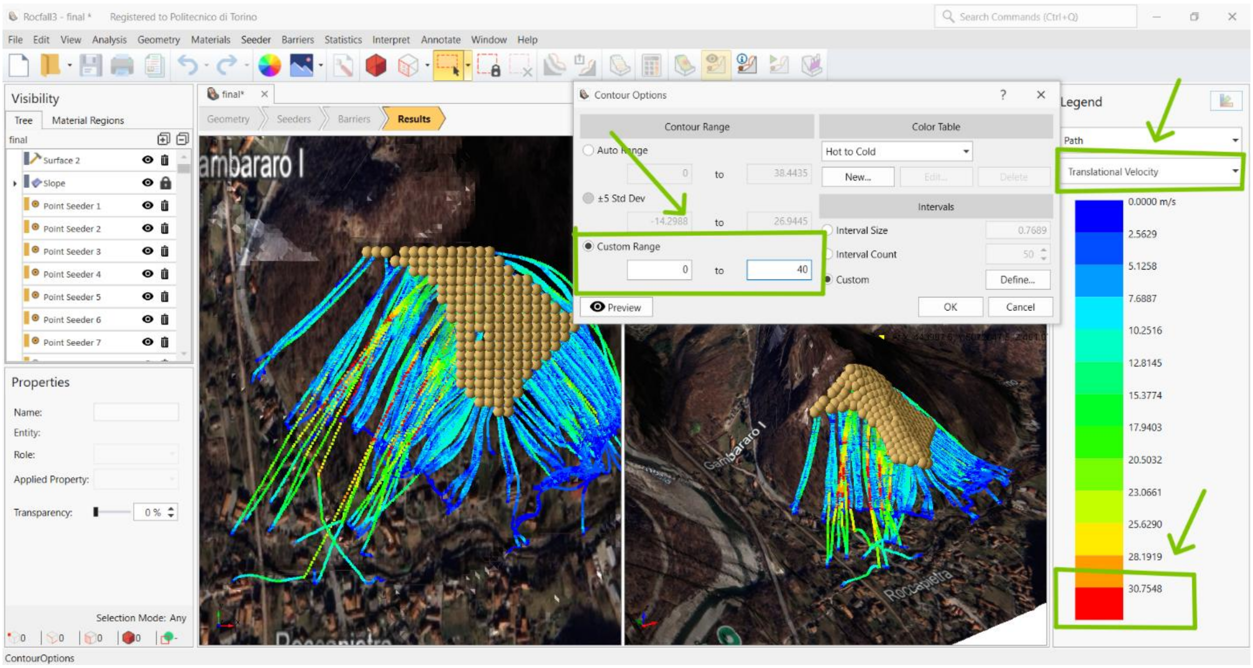

***Figure 38**. Translational Velocity in Rocfall 3D*

6. Conclusion

The comparative analysis clearly shows that **Rocfall 3D** and **Rockyfor3D** provide *coherent and mutually reinforcing* descriptions of rockfall behaviour at the Varallo slope.
Both modelling approaches consistently identify the **southwestern sector** as the most hazardous portion of the site, where the highest translational velocities and kinetic-energy values are concentrated.

Using the same design block volume (**5.4 m^3**), the two models yield highly compatible results. Rocfall 3D predicts a **maximum kinetic energy of about 3.5 MJ** and peak velocities of **30–31 m/s**, values that match the high-energy zones highlighted in the Rockyfor3D simulations.
This close agreement indicates that the physical parameters adopted for the Rocfall 3D analysis are well calibrated and consistent with independent modelling.

Overall, these findings confirm that **Rocfall 3D successfully reproduces the kinematic behaviour observed during the 2023 rockfall event**, providing a reliable basis for future hazard assessments and the design of protective structures in the Varallo area.
Despite the conceptual differences between the two software tools, the strong convergence in both energy and velocity results increases the confidence in the adopted methodology and confirms the robustness of the three-dimensional modelling approach.

References

[1] Napoli, M.L., Barbero, M., Milan, L., & Cavagnino, G. (2025). Validation of the Rockfall SIF and SAI Indexes by a 3D Analysis of a Rock Slope in Valsesia Valley (Italy).
EUROCK 2025 – Rock Mechanics for Sustainable Infrastructure, Trondheim, Norway.

[2] Milan, L., Napoli, M.L., Barbero, M., & Castelli, M. (2023). A Novel Approach to Assess the Influence of Rockfall Source Areas: The Case Study of Bardonecchia (Italy). Geosciences, 13(12), 386. https://doi.org/10.3390/geosciences13120386

[3] Yadav, V., Kainthola, A., Pandey, V.H.R., & Singh, T.N. (2024). Discontinuity-Induced Partial Instability in Markundi Hills, Sonbhadra, Uttar Pradesh, India. Arabian Journal of Geosciences, Springer.

[4] Hoek, E., & Bray, J.W. (1981). Rock Slope Engineering (3rd ed.). London: Institution of Mining and Metallurgy.

[5] Dorren, L.K.A. (2016). Rockyfor3D (V5.2): A Model for Spatially Distributed Rockfall Hazard and Risk Assessment. EcorisQ Association, Zurich.

[6] Rocscience Inc. (2023). Rocfall 3 – 3D Rockfall Analysis Software, User's Guide. Toronto, Canada: Rocscience Inc.

[7] Rocscience Inc. (2020). Rocfall 2 – Two-Dimensional Rockfall Analysis Program, Version 8.0, User's Manual. Toronto, Canada.

[8] s314048 (2023). Rockfall Analysis and Design of Protective Structures Using Rocfall 2. MSc Thesis, Politecnico di Torino, DIATI Department.

[9] Springer Nature. (2025). Arabian Journal of Geosciences – Official Journal Page. Retrieved November 2025, from https://link.springer.com/journal/12517

[10] Cavagnino, G. (2023). Tavola 2 – Energia cinetica (kJ), verifica a ritroso dell'evento franoso del 16 novembre 2023.
Analisi tecnica del dissesto, scala 1:2000. Documento tecnico, Varallo (VC), Italia.

[11] Cavagnino, G. (2023). *Tavola 4* – Energia cinetica (kJ), analisi degli scendimenti potenziali per un volume di 5.4 m^3.
Analisi tecnica del potenziale di propagazione, scala 1:2000. Documento tecnico, Varallo (VC), Italia.